



SAND TRANSPORT IN TIDAL FLOW

by L.C. van Rijn

Content

- 1. Introduction**
- 2. Tidal flow in prismatic and converging channels**
- 3. Salinity intrusion and salinity-induced flow in prismatic and converging tidal channels**
 - 3.1 Salinity intrusion**
 - 3.2 Residual flow velocity**
- 4. Sand transport in tidal flow**
 - 4.1 Sand transport capacity in quasi-steady flow**
 - 4.2 Sand transport in non-steady flow**
 - 4.2.1 Effect of time lags**
 - 4.2.2 Effect of salinity stratification**
 - 4.2.3 Effect of neap-spring tidal cycle**
 - 4.2.4 Effect of mud**
- 5. Quasi-steady 1D sand transport model for tidal flow (TSAND.xls)**
 - 5.1 Definitions**
 - 5.2 Tidal water levels, flow and asymmetry**
 - 5.3 Velocity profile**
 - 5.4 Sand concentrations**
 - 5.5 Sand transport**
 - 5.6 Suspended mud load and transport**
 - 5.7 Example computations**
 - 5.7.1 River flow over sand bed**
 - 5.7.2 Tidal flow over sand-mud bed**
- 6. Time-dependent 2DV sediment transport model for tidal flow (SUSTIM2DV.xls)**
 - 6.1 General**
 - 6.2 Flow field**
 - 6.3 Basic sediment equations**
 - 6.4 Modelling of sand concentrations, transport and bed level changes**
 - 6.4.1 Case 1: Sand concentration profiles in current and wave conditions**
 - 6.4.2 Case 1: Sand transport in tidal channel, Eastern Scheldt, The Netherlands**
- 7. References**



SAND TRANSPORT IN TIDAL FLOW by L.C. van Rijn

1. Introduction

This note is focused on the description of the local, time-dependent sediment transport over a mixed sand-mud bed (mud fraction <30%) in tidal conditions including salinity effects.

The sediment transport equations are implemented in the quasi-steady sand transport model TSAND.xls and in the time-dependent model SUSTIM2DV, see Chapter 4.

Tide-induced and salinity-induced flow are briefly discussed in Chapters 2 and 3.

2. Tidal flow in prismatic and converging channels

An estuary is the (widened) outlet of a river to the sea and is governed by oscillating tidal flow coming from the (saline) sea and by the quasi-steady (fresh) water flow coming from the river in a complicated hydraulic system consisting of channels and shoals. The width and the area of the cross-section reduce in upstream (landward) direction with a river outlet at the end of the estuary resulting in a converging (funnel-shaped) channel system, see **Figure 2.1**. The bottom of the tide-dominated section is almost horizontal. Often, there is a mouth bar at the entrance of the estuary. Tidal flats or islands may be present along the estuary (deltas). The horizontal and vertical tide of this non-linear system can only be solved by a numerical model.

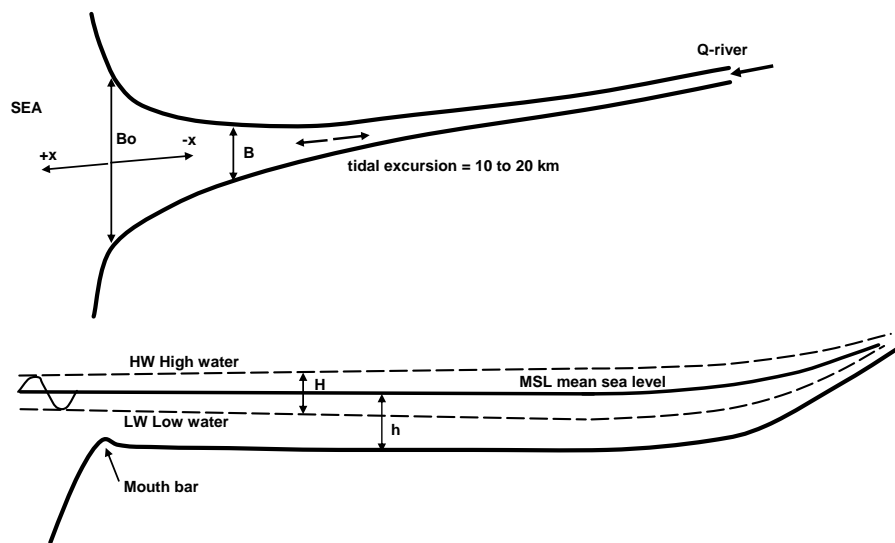


Figure 2.1 Tidal estuary (plan shape and longitudinal section)

The tidal range ($H = 2 \hat{\eta}$) in estuaries is affected by three dominant processes:

- shoaling or amplification due to the decrease of the width in landward direction,
- damping due to bottom friction,
- (partial reflection) at landward end of the estuary.

As a result of these processes there is a phase difference between the vertical (water levels) and horizontal (currents) tide. The horizontal tide has a phase lead of about 1 to 3 hours with respect to the vertical tide.

The variation of the tidal range H along the estuary can be, as follows:

- tidal range is constant $H = H_0$ (defined as an **ideal** estuary);
- tidal range increases $H > H_0$ (**amplified** estuary);
- tidal range decreases $H < H_0$ (**damped** estuary; weakly converging and prismatic channels).



with: H = tidal range and H_o = tidal range at entrance (mouth).

The offshore astronomical tide is composed of various constituents. The most important constituent is the semi-diurnal M_2 -component. The first harmonic of this constituent is M_4 . Generally, the M_4 -component is small offshore, but rapidly increases within estuaries due to bottom friction and channel geometry. The M_2 -component and its first harmonic M_4 dominate the non-linear processes within estuaries. Non-linear interaction between other constituents is also possible in shallow estuaries.

Analysis of field observations has shown that interaction of M_2 and its first harmonic M_4 explains the most important features of tidal asymmetries. The type of tidal distortion (flood or ebb dominance) depends on the relative phasing of M_4 to M_2 .

The equations of continuity and motion for 1-dimensional depth-averaged flow in a converging tidal channel with a regular cross-section are given by:

$$\frac{b \partial \eta}{\partial t} + \frac{\partial Q}{\partial x} = 0 \quad (2.1)$$

$$\frac{1}{A} \frac{\partial Q}{\partial t} + \frac{g \partial \eta}{\partial x} + \frac{Q |Q|}{C^2 A^2 R} = 0 \quad (2.2)$$

in which: $A = b h_o$ = cross-section area, b = width, h_o = depth to mean sea level, R = hydraulic radius and C = Chézy-coefficient are constants.

Basically, this set of non-linear equations can only be solved by a numerical model.

An analytical solution of the mass and momentum balance equations can also be obtained (Van Rijn, 2011) for a converging (funnel type) channel, if it is assumed that the:

- bottom is horizontal ($l_b = 0$);
- channel depth to MSL is constant in space and time ($h = h_o + \eta$); depth h_o = constant;
- width $b = b_o e^{\beta x}$ with $\beta = 1/L_b$ = convergence coefficient, L_b = converging length scale, constant in time;
- convective acceleration ($\bar{u} \partial \bar{u} / \partial x = 0$) is neglected;
- friction is linear;
- fluid density is constant.

The solution reads as:

$$\eta = \hat{\eta}_o e^{(-0.5\beta + \mu)x} \cos(\omega t + kx) = \text{tidal water level} \quad (2.3)$$

$$\bar{u} = \hat{u}_o e^{(-0.5\beta + \mu)x} \cos(\omega t + kx + \varphi) = \text{tidal velocity (cross-section averaged value)} \quad (2.4)$$

$$\begin{aligned} \hat{\eta}_o &= -h_o \hat{u}_o (k/\omega)(1/\cos\varphi) = \text{peak tide amplitude at mouth } x=0 \\ \hat{u}_o &= -(\hat{\eta}_o/h_o)(c) \cos\varphi = \text{peak tidal velocity at mouth} \end{aligned} \quad (2.5)$$

$$\tan\varphi = (0.5\beta + \mu)/k \quad (2.6)$$

x = negative in landward direction, k = wave number and μ = friction parameter, $c = \omega/k$ = wave speed, with $\beta = 1/L_b$ = convergence coefficient, $\beta = 0$ for prismatic channel, φ = phase shift between horizontal and vertical tide.



3. Salinity intrusion and salinity-induced flow in prismatic and converging tidal channels

3.1 Salinity intrusion

The most simple approach for determining the salinity distribution and the salt intrusion length in an estuary with river inflow is to use a cross-section-averaged and tide-averaged (1-dimensional) approach. This is most valid for **well-mixed conditions** (ρ is constant in vertical direction). Landward salt water intrusion in well-mixed conditions is caused by advective-type and dispersive-type of processes. When the river discharge remains constant for some time (\gg Tidal period), the salt penetration length will become constant on a tide-averaged time scale. The tide-averaged salt penetration length will decrease for increasing fresh water discharge and increase for decreasing discharge.

Figure 3.1.1 shows various types of cross-section averaged salt concentration distributions in a tidal estuary. The lower exponential distribution (—) is a concave distribution (rounded inward) and mainly occurs in prismatic estuaries. The upper distribution (— . —) is a convex-type of distribution (rounded outward) and occurs in large estuaries with a small river at the landward side (Western Scheldt Estuary, The Netherlands; Thames Estuary, England).

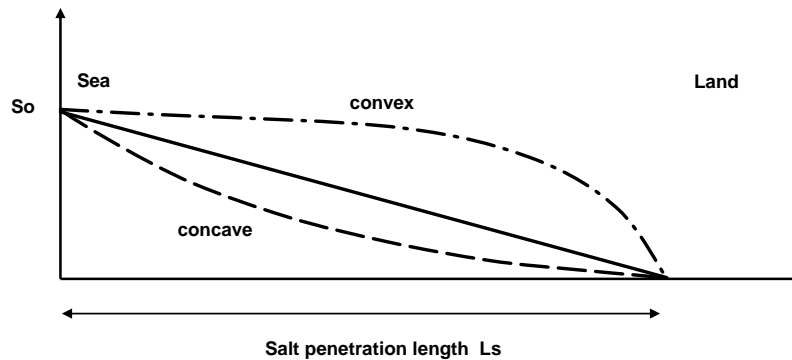


Figure 3.1.1 Various types of salt concentration distributions in a tidal estuary

Averaging the salt transport terms over the cross-section and over time yields the balance equation for advective seaward salt transport and dispersive landward salt transport in stationary conditions (river discharge should be constant for some time, say 10 days), as follows (Van Rijn 2011):

$$u_r \langle S \rangle - D \langle \partial S / \partial x \rangle = 0 \quad (3.1)$$

with: u_r = cross-section averaged velocity based on river discharge ($= Q/A$; negative in seaward direction), S = cross-section averaged salt concentration (kg/m^3), D = dispersion coefficient, Q = river discharge (fresh water), $A = b h$ = area of cross-section, b = average width of cross-section, $h = h_0$ = average water depth to mean water level (assumed to be constant), $\langle \dots \rangle$ = time-averaged value (averaged over the tidal period T).

The salinity in an estuary channel can only be represented by the cross-section-averaged salinity if the lateral mixing proceeds relatively fast within the tidal cycle, which means that the channel width should be small compared with the channel length and width variations should be gradual.

The time-dependent salt balance equation can be formulated as (Van Rijn, 2011):

$$\partial S / \partial t + (u_{\text{tide}} - u_r) \partial S / \partial x - D_s (\partial^2 S / \partial x^2) = 0 \quad (3.2)$$

with: u_{tide} = tidal velocity (flood= positive; ebb= negative),
 u_r = fresh water velocity based on river discharge (negative in seaward direction).



The time-dependent solution can be described, as (Van Rijn, 2011):

$$S_{x,t}/S_0 = [1 - \{x + x_b - (0.5L_e) + (0.5L_e) \cos(\omega t)\}/(x_b + L_{s,min})]^2 \quad (3.3)$$

Assuming $x_b \ll L_{s,min}$, it follows that:

$$S_{x,t}/S_0 = [1 - \alpha_x + 0.5\beta (1 - \cos(2\pi t/T))]^2 \quad (3.4)$$

with: $\alpha_x = (x + x_b)/L_{s,min}$, $\beta = L_e/L_{s,min}$, x = location inside estuary from the mouth ($x=0$), L_e = tidal excursion = $U_{max} T/\pi$ and $L_{s,min}$ = minimum tidal excursion at low water slack tide = $D_0/(0.5 u_r)$, D_0 = dispersion coefficient at mouth in the range of 500 to 1500 m²/s and x_b = horizontal distance (positive value $x \cong 150 h_0$) of the sea boundary seaward of the mouth ($x=0$), T = tidal period.

If $\alpha_x - 0.5\beta (1 - \cos(2\pi t/T)) \leq 0$ then $S = S_0$.

If $\alpha_x - 0.5\beta (1 - \cos(2\pi t/T)) \geq 1$ then $S = 0$.

The maximum salt intrusion length is: $L_{s,max} = L_{s,min} + L_e$

The salinity and fluid density is computed as: $\rho = \rho_{fresh} + 0.77 S = 1000 + 0.77 S$.

Equation (3.4) is implemented in the TSAND.xls model.

3.2 Residual flow velocity

Due to gravitational circulation a residual flow is generated in a tidal channel with fresh water inflow. The residual flow is landward near the bottom and seaward near the water surface. The point where the tide-averaged flow velocity near the bottom is approximately zero is known as the **null point**.

Residual density-induced flow in a prismatic channel with tidal conditions can be determined by using the tide-averaged momentum equation. There are two main contributions: the free convection contribution arising from the density difference between salt water and fresh water and the fresh water discharge contribution.

Assuming well-mixed conditions and relatively small inertial terms (after averaging over the tidal cycle), the tide-averaged continuity and momentum equations for two-dimensional vertical flow in a prismatic channel with rectangular cross-section (width \gg depth) can be easily formulated (Van Rijn, 2011)

Assuming reasonably well-mixed conditions, the residual flow velocity profile can be expressed as:

$$u_{s,z} = M h_0^2 \left[- (1/6) (z/h_0)^3 + (1/2) (z/h_0)^2 - (1/4) (z/h_0) \right] \quad (3.5)$$

$$M = [g^{0.5} C / \{\gamma (|U_{max}| + |\bar{u}_r|) h_0\}] [(h_0/\rho_{fresh}) (\partial\rho/\partial x)]$$

with: z = level above bed (m), h = water depth at time t , h_0 = tide-averaged water depth (m), er level (m), $u_r = Q/(bh)$ = river velocity, $z_0 = 0.033k_{s,c}$ = zero-velocity level, $k_{s,c}$ = current-related bed roughness (wave-current interaction is neglected), M = salinity factor, C = Chézy-coefficient at time t , ρ_{sea} = density of sea water (kg/m³), $\partial\rho/\partial x$ = salinity-induced horizontal density gradient (input value; about 0.001 or 1 kg/m³ per 1 km in stratified flow), ρ = depth-averaged and tide-averaged fluid density due to salinity = $\rho_{fresh} + 0.77 S_a$ (kg/m³), ρ_{fresh} = fresh water density, S = salinity (0 to 25 kg/m³), γ = coefficient (about 0.005 to 0.01).

The maximum residual velocity is approximately: $u_{s,max} = -0.035 M h_0^2$ about $z/h_0 = 0.3$.



4. Sand transport in tidal flow

4.1 Sand transport capacity in quasi-steady flow

The sediment transport capacity formulae of Engelund-Hansen (1967) and Van Rijn (1984) which are most valid for steady-state conditions (river flow conditions), yield reasonably good results in tidal conditions for bed material sizes larger than about 0.3 mm, see Voogt et al. 1991 and Van Rijn 1993. These formulae tend to slightly overpredict for accelerating conditions and underpredict for decelerating conditions, which is related to the time lag effect. The formula of Engelund-Hansen has no initiation of motion effect and can therefore not be used in conditions with sand-mud mixtures. The transport capacity formulae give inaccurate results when the salinity-related damping effect is significant (vertical density gradient in stratified flow)

4.2 Sand transport in non-steady flow

4.2.1 Effect of time lags

In non-steady flow the actual sediment transport rate may be smaller (underload) or larger (overload) than the transport capacity resulting in net erosion or deposition assuming sufficient availability of bed material (no armour layers).

Bed-load transport in non-steady flow can adjust rapidly to the new hydraulic conditions, but suspended load transport, however, needs time to adjust because the particles are carried upwards and downwards over the water depth.

Tidal flow is characterized by a daily ebb and flood cycle with a time scale of 6 to 12 hours (semidiurnal or diurnal tide) and by a neap-spring cycle with a time scale of about 14 days.

Sediment concentration measurements in tidal flow over a fine sand bed (0.05 to 0.3 mm) show a continuous adjustment of the concentrations to the flow velocities with a lag period in the range of 0 to 60 minutes

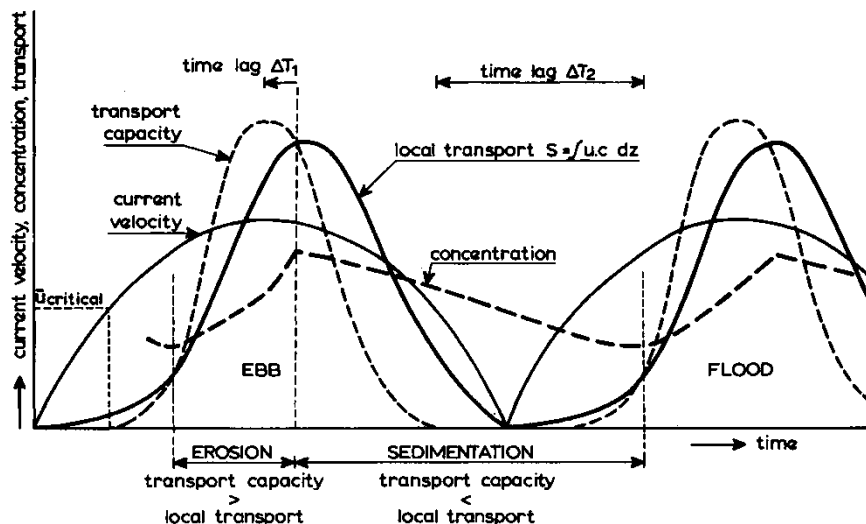


Figure 4.1 Time lag of suspended sediment concentrations in tidal flow

These basic transport processes in tidal flow are shown in **Figure 4.1**. Sediment particles go into suspension when the current velocity exceeds a critical value. In accelerating flow there always is a net vertical upward transport of sediment particles due to turbulence-related diffusive processes, which continues as long as the sediment transport capacity exceeds the actual transport rate. The time lag period ΔT_1 is the time period between the time of maximum flow and the time at which the transport capacity is equal to the actual



transport rate. After this latter time there is a net downward sediment transport because settling dominates yielding smaller concentrations and transport rates. In case of very fine sediments (silt) or a large depth, the settling process can continue during the slack water period giving a large time lag (ΔT_2) which is defined as the period between the time of zero transport capacity and the start of a new erosion cycle. **Figure 4.1** shows that the suspended sediment transport during decelerating flow is always larger than during accelerating flow.

4.2.2 Effect of salinity stratification

In a stratified estuary a high-density salt wedge exists in the near-bed region resulting in relatively high near-bed densities and relatively low near-surface densities. The horizontal density-gradient generates a net tide-averaged landward flow near the bed and seaward flow near the surface. Stratified flow will result in damping of turbulence because turbulence energy is consumed in mixing of heavier fluid from a lower level to a higher level against the action of gravity.

The usual method to account for the salinity-related stratification effect on the velocity and concentration profiles is the reduction of the fluid mixing coefficient by introducing a damping factor related to the Richardson-number (Ri), as follows: $\varepsilon_f = \phi \varepsilon_{f,0}$ with $\varepsilon_{f,0}$ =fluid mixing coefficient in fresh water, $\phi = F(\text{Ri})$ = damping factor (< 1), Ri = local Richardson number.

Termes (1990) studied the influence of the vertical density gradient on the sand concentration profile. Three different density profiles were considered: L-, S- and J-profiles. The L-density profile represents a linear distribution between the bed density of 1020 kg/m^3 and the surface density of 1000 kg/m^3 . The ϕ -factor was represented by a function given by Munk-Anderson: $\phi = (1 + 3.3 \text{ Ri})^{-1.5}$.

Based on these input variables, the concentration profiles for particles of 0.2 mm were computed for fresh water (no salinity gradient) and for stratified conditions (L-, S- and J-density profiles). The results in **Figure 4.2** show a considerable reduction of the concentrations due to damping of turbulence. The influence is largest for the J-density profile and smallest for the S-density profile.

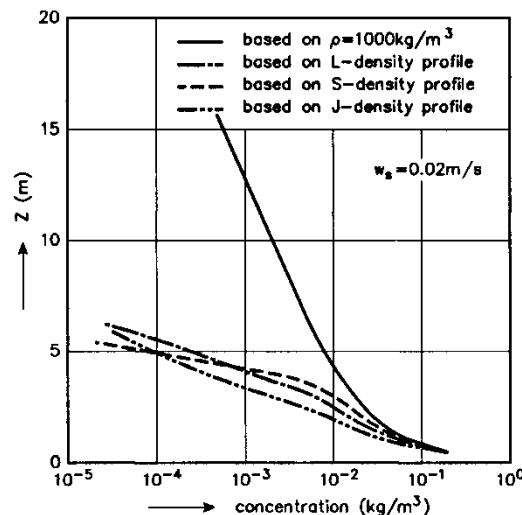


Figure 4.2.2 Sand concentration profiles (Termes, 1990)



4.2.3 Effect of neap-spring tidal cycle

The tidal range of the neap-spring tidal cycle varies as a function of time which is mainly caused by astronomical effects. Apart from astronomical effects, there are also climatological effects (wind effects) which are superimposed on the astronomical variations.

Sand transport computations in tidal conditions requires representation of the neap-spring cycle. This can be simply done by multiplying the velocities of the *mean tidal cycle* by a (correction) factor ζ to account for the higher velocities and hence higher transport rates (power-law relationship of transport and velocity) during springtide conditions.

The correction factor varies roughly between $\zeta = 1.05$ and 1.1 for $H_{\max}/H_{\text{mean}} = 1.2$ to 1.4 with H_{\max} = maximum tidal range in neap-spring cycle and H_{mean} = mean tidal range of neap-spring cycle. Details of this method are given by Van Rijn (1993).

4.2.4 Effect of mud

In most tidal basins the sediment bed consists of a mixture of sand and mud. The sand-mud mixture generally behaves as a mixture with cohesive properties when the mud fraction (all sediments < 0.05 mm) is dominant ($p_{\text{mud}} > 0.3$) and as a non-cohesive mixture when the sand fraction is dominant ($p_{\text{sand}} > 0.7$). The distinction between non-cohesive mixtures and cohesive mixtures can be related to a critical mud content ($p_{\text{mud,cr}}$). Most important is the value of the clay/lutum-fraction (sediments < 0.005 mm) in the mixture. Cohesive properties become dominant when the clay-fraction is larger than about 0.05 to 0.1. Assuming a clay-mud ratio of 0.5 to 0.25 for natural mud beds, the critical mud content will be about $p_{\text{mud,cr}} = 0.2$ to 0.4 .

If the mud content is below the critical value ($p_{\text{mud}} < p_{\text{mud,cr}}$), the sand-mud mixture is herein assumed to be homogeneous with depth and to have non-cohesive properties. Furthermore, the erosion of the sand particles is the dominant erosion mechanism. The mud particles will be washed out together with the sand particles. Laboratory and field observations (Van Rijn, 1993 and Van Ledden, 2003) have shown that the erosion of the sand particles is slowed down by the presence of the mud particles. This behaviour can be quite well modelled by increasing the critical bed-shear stress for initiation of motion of the sand particles. Herein, it is assumed that: $\tau_{b,cr,sand} = (1 + p_{\text{mud}})^{\beta} \tau_{b,cr,shields}$ with $\beta = 3$ based on analysis of field data.



5. Quasi-stationary 1D sand transport model for tidal flow (TSAND.xls)

5.1 Definitions

The TSAND.xls model can be used to compute the variation of the depth-integrated suspended sand transport and total sand transport (incl. bed-load transport) in a single point over the tidal cycle. The mud transport is included assuming that the sediment bed ($\rho_{mud} + \rho_{sand} = 1$) behaves as a non-cohesive or weakly cohesive mixture. The velocities and sand concentrations are computed as a function of z and t ; z =height above bed and t =time (fixed time step of 5 min). The grid points over the depth (20 points) are distributed according to an exponential function, as follows:

$$z = a[h/a]^{(k-1)/(N-1)} \quad (5.1)$$

with: a = reference height above bed (input value), $h = h_o + \eta$ = water depth, h_o = depth between bed and mean sea level, η = tidal water level, k = index number of point k , N = total number of grid points (=20).

5.2 Tidal water levels, flow and asymmetry

The tidal water level at each time t is represented, as:

$$\begin{aligned} \eta_{flood,t} &= \eta_{flood,max} \sin\{\pi(t-\Delta T)/T_{flood}\} & \text{for } t < T_{flood} & \quad (5.2) \\ \eta_{flood,max} &= f_a (H/2) \\ T_{flood} &= (\eta_{ebb,max}/H)T \end{aligned}$$

$$\begin{aligned} \eta_{ebb,t} &= \eta_{ebb,max} \sin\{\pi(t-T_{flood}-\Delta T)/T_{ebb}\} & \text{for } t > T_{flood} & \quad (5.3) \\ \eta_{ebb,max} &= -(1/f_a)(H/2) \\ T_{ebb} &= (\eta_{flood,max}/H)T \end{aligned}$$

with: H = tidal range tidal water level (input value); f_a = asymmetry factor (input value=1 tot 1.2, $f_a=1$ yields a symmetrical tide), T = tidal period (input value), ΔT = phase shift (seconds; velocity is ahead of water level), T_{flood} = flood period, T_{ebb} = ebb period.

The depth-averaged velocity at each time t is represented, as:

$$\begin{aligned} u_t &= u_r + u_{flood,max} \sin(\pi t/T_{flood}) & \text{for } t < T_{flood} & \quad (5.4) \\ u_{flood,max} &= f_a (U_{max}) \end{aligned}$$

$$\begin{aligned} u_t &= u_r + u_{ebb,max} \sin\{\pi(t-T_{flood})/T_{ebb}\} & \text{for } t > T_{flood} & \quad (5.5) \\ u_{ebb,max} &= -1/f_a (U_{max}) \end{aligned}$$

with: u_t =depth-averaged velocity at time t (m/s), u_r = net tide-averaged and depth-averaged velocity = $Q/(b h)$, b = flow width of channel (input value), h = water depth (input value), $U_{max} = (u_{flood,max} + u_{ebb,max})/2$ (input value).

5.3 Velocity profile

The vertical distribution of the velocity at each time t is represented, as:

$$u_{z,t} = u_{s,z} + [u_t/(-1+\ln(h/z_o))] \ln(z/z_o) \quad (5.6)$$



with: $u_{s,z}$ = residual flow velocity due to horizontal salinity-induced density gradient based on Equation (3.2.1), z = level above bed (m), h = water depth at time $t = h_o + \eta_t$ (m), h_o = tide-averaged water depth (m), η_t = tidal water level (m), u_t = depth-averaged flow velocity at time t due to tide + steady river current (m/s), $u_r = Q/(bh)$ = river velocity, $z_o = 0.033k_{s,c}$ = zero-velocity level, $k_{s,c}$ = current-related bed roughness (wave-current interaction is neglected).

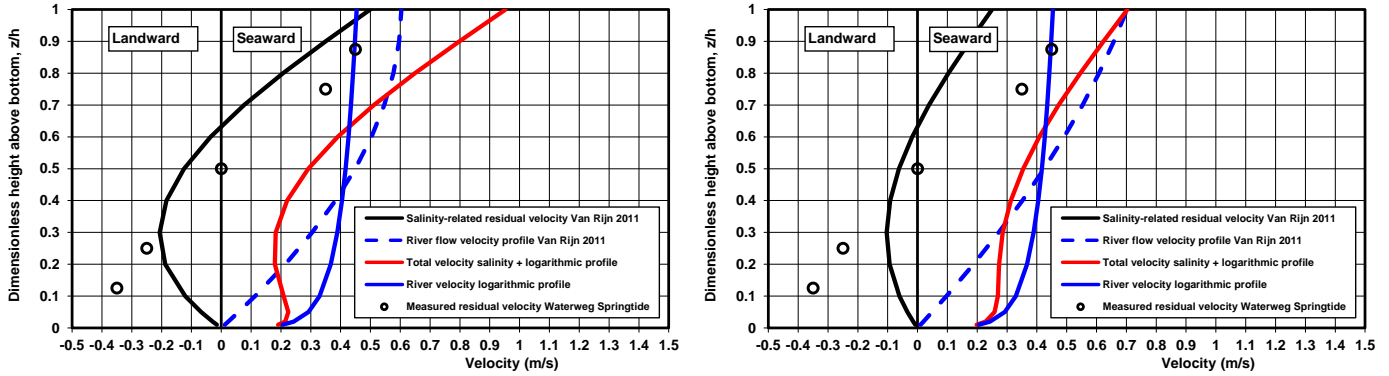


Figure 5.1 River velocity plus salinity-induced residual flow velocity profile
Left: $\gamma = 0.005$ and Right: $\gamma = 0.01$

The first part of Equation (5.6) represents the residual flow due to the density gradient. The depth-integration yields zero flow velocity. The second part represents the river flow velocity profile due to fresh water discharge.

Figure 5.1 show the residual flow velocity profile for h_o = water depth= 15 m, u_r = river velocity= 0.4 m/s, $k_{s,c}$ =bed roughness= 0.1 m, $\rho_{sa} = 1025 \text{ kg/m}^3$, $\partial\rho_{sa}/\partial x = 0.001$. Two values of the γ -coefficient (0.005 and 0.01) have been used. Measured salinity-related residual flow velocities during the springtide of October 1975 in the Nieuwe Waterweg near Rotterdam are also shown. The agreement is best for $\gamma = 0.005$. Two velocity profiles are shown for the steady river velocity. The logarithmic velocity profile is preferred and is implemented in the TSAND-model. The salinity-induced flow reduces the near-bed river flow velocity, but increases the river flow velocity near the water surface. The near-bed velocity at $z \cong 0.1 h$ is used to compute the bed-shear stress.

5.4 Sand concentrations

The sand concentrations are computed using a single fraction and a multi-fraction method.

The multi-fraction method is based on $N=6$ sand fractions (0.062-0.125 mm, 0.125-0.2 mm, 0.2-0.3 mm, 0.3-0.5 mm, 0.5-1 mm, 1-2 mm).

The sand concentration profile at each time t is represented, as:

$$\text{Single fraction: } c_{sand} = c_{a,sand} \left[\left(\frac{h-z}{z} \right) \left(\frac{a}{h-a} \right) \right]^{ZS} \quad (5.7a)$$

$$\text{Multi fraction: } c_{sand,i} = c_{a,sand,i} \left[\left(\frac{h-z}{z} \right) \left(\frac{a}{h-a} \right) \right]^{ZS_i} \quad (5.7b)$$

with: c_{sand} = sand concentration (kg/m^3), $c_{a,sand}$ = reference sand concentration (kg/m^3), ZS = suspension number of sand (-), ZS_i = suspension number of sediment fraction i .

The reference concentration c_a of the sand fraction is represented, as:

$$\text{Single fraction: } c_{a,sand} = 0.015 \alpha_{ca} (1-p_{mud}) (d_{50}/a) (T)^{1.5} (D^*)^{-0.3} \quad (5.8a)$$

$$\text{Multi fractions: } c_{a,sand,i} = 0.015 \alpha_{ca} (1-p_{mud}) (d_i/a) (T_i)^{1.5} (D^*_{,i})^{-0.3} \quad (5.8b)$$



with: α_{ca} = correction coefficient (default=1), d_{50} = median particle diameter,
 $D^* = d_{50}[(s-1)g/v^2]^{0.333}$ = dimensionless particle parameter, $D^*_{*,i}$ = particle parameter of fraction i,
 $T = (\tau_b'/\chi\tau_{b,cr})/\chi\tau_{b,cr}$ = dimensionless bed-shear stress parameter,
 $T_i = [\lambda_i(\tau_b'/\chi\tau_{b,cr,d50})]/[\chi(d_i/d_{50})\tau_{b,cr,d50}]$ = dimensionless bed-shear stress parameter of fraction i,
 $\tau_{b,cr,d50}$ = critical bed-shear stress of sand based on d_{50} ,
 $\tau_b' = \mu_c\tau_{b,c} + \mu_w\tau_{b,w}$ = effective bed-shear stress due to current and waves, $s = \rho_s/\rho$ = relative density,
 $\chi = (1 + p_{gravel})(1 + p_{mud})^3$ = factor representing effect of mud on the critical shear stress of sand,
 $\lambda_i = (d_i/d_{50})^{0.25}$ = roughness correction factor of fraction i,
 $\zeta_i = (d_{50}/d_i)^{0.5}$ = hiding-exposure factor of fraction i (maximum 2 and minimum 0.5),
 v = kinematic viscosity coefficient, ρ_s = sediment density (input value), ρ = fluid density,
 p_{mud} = fraction of mud (<0.062 mm) of top layer of bed (0 to 0.3),
 p_{gravel} = fraction of gravel (> 2 mm) of top layer of bed (0 to 0.1).

The critical bed-shear stress of Shields (with d_{50}) is represented by: $\tau_{b,cr} = (\rho_s - \rho) g d_{50} [0.24/D^* + 0.055(1 - e^{-0.02D^*})]$

The bed-shear stresses at time t due to currents and waves are represented as:

$$\tau_{b,c} = \rho (u^*_{*,c})^2 \quad (5.9)$$

$$u^*_{*,c} = \kappa u_z / \ln(30z/k_{s,c})$$

with: $\kappa = 0.4$ and u_z = flow velocity at $z \cong 0.1 h$ (velocity of layer 12).

$$\tau_{b,w} = 0.25 \rho f_w (U_w)^2 \quad (5.10)$$

with: $U_w = (2\pi/T_p)A_w$ = peak orbital velocity (linear wave theory), A_w = peak orbital excursion, T_p = peak wave period, $f_w = \exp(-6 + 5.2(A_w/k_{s,w})^{-0.19})$ = wave-related friction coefficient, ρ = fluid density including salinity effect; $k_{s,c}$ = current-related roughness, $k_{s,w}$ = wave-related roughness.

The effective bed-shear stresses at time t for sediment transport are represented as:

$$\tau_{b,c}' = \mu_c \tau_{b,c} \quad (5.11)$$

$$\tau_{b,w}' = \mu_w \tau_{b,w} \quad (5.12)$$

$\mu_c = f_c'/f_c$ = current-related efficiency factor, $f_c = 0.24/(\log(12h/k_{s,c}))^2$ = current-related friction coefficient, $f_c' = 0.24/(\log(12h/d_{90}))^2$ = grain-related friction coefficient, d_{90} = grain size.

$\mu_w = 0.7/D^*$ = wave-related efficiency factor ($\mu_{w,min} = 0.14$, $\mu_{w,max} = 0.35$ based on d_{50}).

The suspension number ZS of sand is represented as:

$$\text{SF: } ZS = w_{sand,o}/(\beta\kappa u^*_{*,cw}) + 2.5(w_{sand,o}/u^*_{*,cw})^{0.8}(c_{a,sand}/c_o)^{0.4} + (\rho_{sa}/\rho_{fresh} - 1)^{0.4} \quad (5.13a)$$

$$\text{MF: } ZS_i = w_{sand,i,o}/(\kappa u^*_{*,cw}) + 2.5(w_{sand,o}/u^*_{*,cw})^{0.8}(c_{a,sand}/c_o)^{0.4} + (\rho_{sa}/\rho_{fresh} - 1)^{0.4} \quad (5.13b)$$

with: $w_{sand,o}$ = fall velocity of single sand particle based on d_{50} , $w_{sand,i,o}$ = fall velocity of fraction i, $\kappa = 0.4$, $\beta = 1 + 2(w_{sand,o}/u^*_{*,cw})^2$ = coefficient ($\beta_{max} = 1.5$), $u^*_{*,cw} = (u^*_{*,c}{}^2 + u^*_{*,w}{}^2)^{0.5}$ = bed-shear velocity due to current and waves, $u^*_{*,c} = (\tau_{b,c}/\rho)^{0.5}$ = current-related bed-shear stress, $u^*_{*,w} = (\tau_{b,w}/\rho)^{0.5}$ = wave-related bed-shear stress, $c_{a,sand}$ = total reference concentration, $c_o = 0.65$ = maximum bed concentration, ρ_{sa} = fluid density including salinity effects, ρ_{fresh} = fluid density of fresh water (= 1000 kg/m³).

Equation (5.13) represents the effects of downward gravity settling, upward turbulence mixing (first term), damping due to vertical sediment concentration gradients (second term) and damping due to vertical salinity gradients (third term). The damping due to vertical salinity/density gradients mainly occurs during the flood period when the salt wedge penetrates landward (last term of Eq. 5.13 only during flood). A larger ZS-value yields smaller concentrations during flood. This latter effect is only relevant in conditions with a longitudinal salinity gradient.



The time lag effect of the suspended sand concentrations rate can be (crudely) computed by applying an exponential adjustment of the reference concentration at time t based on $dc_a/dt = -A(C_{a,t} - C_{a,t,eq})$, resulting in:

$$C_{a,sand,t} = C_{a,sand,t-\Delta t} + dC_{a,sand} \quad (5.14)$$

$$C_{a,sand,t} = C_{a,sand,t-\Delta t} + [-A(C_{a,sand,t} - C_{a,sand,t,eq})\Delta t] \quad (5.15)$$

$$C_{a,sand,t} = [1/(1 + A \Delta t)] [C_{a,sand,t-\Delta t} + A \Delta t C_{a,sand,t,eq}] \quad (5.16)$$

with: Δt = time step (5 min), $C_{a,sand,t-\Delta t}$ = suspended reference concentration at previous time ($\sum C_{a,i}$ for multifraction method), $C_{a,sand,t,eq}$ = equilibrium reference concentration at time t,
A = coefficient = $\gamma_c 0.05(1/h)(w_{sand,o}/u^*_{cw})(1+2w_{sand,o}/u^*_{cw})(1+H_s/h)^2$, $A_{minimum} = 0.0005$ (based on d_{50}),
 γ_c = calibration coefficient (range 0.5 to 2; default = 1).

5.5 Sand transport

Suspended sand transport

The suspended sand transport q_s can be computed by integration of the product of velocity and concentration over the water depth:

$$SF: \quad q_s = \int_a^h (u C_{sand}) dz \quad \text{with } h = \text{water depth (summation over depth)} \quad (5.17a)$$

$$MF: \quad q_s = \int_a^h \sum^N (u C_{sand}) dz \quad \text{with } N = 6 = \text{number of fractions (summation over fractions)} \quad (5.17b)$$

The suspended load transport is also computed by using a simplified transport capacity formula, as follows:

$$q_s = 0.012 \gamma_s \rho_s (1-p_{mud}) u h M_e^{2.4} (d_{50}/h) (D^*)^{-0.6} \quad (5.18)$$

with:

q_s = suspended load transport (kg/m/s); h = water depth, d_{50} = particle size (m), p_{mud} = percentage of mud in bed (0 to 0.5); $D^* = d_{50}[(s-1)g/v^2]$ = dimensionless particle size; v = kinematic viscosity coefficient;

$M_e = (u_e - u_{cr}) / ((s-1)gd_{50})^{0.5}$ = mobility parameter; $u_e = u + 0.4U_w$ = effective velocity;

u = depth-averaged flow velocity $\approx 1.2 u_{0.1h}$; $u_{0.1h}$ = velocity at $z = 0.1h$ above the bed;

$s = \rho_s/\rho =$ relative density; $U_w = \pi H_s / (T_p \sinh(kh))$ = peak orbital velocity (based on linear wave theory),

H_s = significant wave height, T_p = peak wave period, $kh = Y^{0.5} [1 + 0.166Y + 0.031Y^2]$ and $Y = 4.02h/T_p^2$;

$u_{cr} = \alpha u_{cr,c} + (1-\alpha)u_{cr,w}$ with $\alpha = u/(u+U_w)$; $U_w = 0$ for no waves; γ_s = calibration coefficient (default=1);

$u_{cr,c}$ = critical velocity for currents based on Shields (initiation of motion); $u_{cr,w}$ = critical velocity for waves; effect of mud included;

$$u_{cr,c} = 0.19(1+p_{mud})^{1.5} (d_{50})^{0.1} \log(12h/3d_{90}) \quad \text{for } 0.0001 < d_{50} < 0.0005 \text{ m;}$$

$$u_{cr,c} = 8.5(1+p_{mud})^{1.5} (d_{50})^{0.6} \log(12h/3d_{90}) \quad \text{for } 0.0005 < d_{50} < 0.002 \text{ m;}$$

$$u_{cr,w} = 0.24(1+p_{mud})^{1.5} ((s-1)g)^{0.66} d_{50}^{0.33} (T_p)^{0.33} \quad \text{for } 0.0001 < d_{50} < 0.0005 \text{ m;}$$

$$u_{cr,w} = 0.95(1+p_{mud})^{1.5} ((s-1)g)^{0.57} d_{50}^{0.43} (T_p)^{0.14} \quad \text{for } 0.0005 < d_{50} < 0.002 \text{ m.}$$

Bed load transport

The bed load transport (in kg/m/s) is computed as:

$$SF: \quad q_b = 0.015 \gamma_s \rho_s (1-p_{mud}) u h M_e^{1.5} (d_{50}/h)^{1.2} \quad (5.19a)$$

$$MF: \quad q_{b,i} = 0.015 \gamma_s \rho_s (1-p_{mud}) u h M_{e,i}^{1.5} (d_i/h)^{1.2} \quad (5.19b)$$

with:

$M_e = (u_e - u_{cr,i}) / ((s-1)gd_i)^{0.5}$ = mobility parameter of fraction i

$$u_{cr,i} = (\zeta_i)^{0.5} u_{cr}$$



Total load transport

The total load transport of sand at each time t is computed as:

$$q_{tot} = q_s + q_b \quad (5.20)$$

with: q_b = bed-load transport according to Equation (5.19).

The total load formula of Engelund-Hansen is also used, as follows:

$$q_{tot, EH} = 0.05 \rho_s u^5 (s-1)^{-2} g^{-0.5} d_{50}^{-1} C^{-3} = 0.05 \rho_s (s-1)^{-2} g^{-3} C^2 (u_{*,c})^5 \quad (5.21)$$

with: $u_{*,c}$ = bed-shear velocity due to tidal flow at time t , C = Chézy-coefficient at time t .

5.6 Suspended mud load and transport

In the case of sand-mud mixtures (percentage sand >70%), the mud load and the mud transport can be determined by assuming that the top layer of the bed is homogeneously mixed and that the mud particles are washed out together with the sand particles. The suspended sand load can be determined as (bed load is neglected):

$$L_{sand} = a \int^h (c_{sand}) dz \quad (5.22)$$

The corresponding layer thickness of eroded sand is:

$$\Delta_s = L_{sand} / (p_{sand} \rho_{b,sand}) \quad (5.23)$$

with: p_{sand} = percentage of sand of bed, $\rho_{b,sand}$ = bulk density of sand fraction (about 1600 kg/m³).

The amount of mud in this layer is:

$$L_{mud} = p_{mud} \rho_{b,mud} \Delta_s = (p_{mud}/p_{sand}) (\rho_{b,mud}/\rho_{b,sand}) L_{sand} \quad (5.24)$$

with: p_{mud} = percentage of mud of bed, $\rho_{b,mud}$ = bulk density of mud fraction (about 800 to 1600 kg/m³).

The mud load is also defined by:

$$L_{mud} = a \int^h (c_{mud}) dz = c_{a,mud} a \int^h (f_z) dz \quad (5.25)$$

with: $f_z = [((h-z)/z)(a/(h-a))]^{ZM}$, $ZM = w_{mud,o} / (\kappa u_{*,cw})$ = suspension number of mud, $w_{mud,o}$ = fall velocity of individual mud particles (flocculation effect is neglected), $u_{*,cw}$ = bed-shear velocity due to currents and waves.

The reference concentration of mud can now be determined as:

$$c_{a,mud} = L_{mud} / a \int^h (f_z) dz = [(p_{mud}/p_{sand}) (\rho_{b,mud}/\rho_{b,sand}) L_{sand}] / [a \int^h (f_z) dz] \quad (5.26)$$

The mud transport can be determined from:

$$q_{mud} = a \int^h (u c_{mud}) dz \quad (5.27)$$

Since the mud load is eroded at the same time as the sand load, the adjustment of the mud concentrations is relatively small and approximately equal to that of the sand load.

The tide-integrated sand transport rates are computed as: $Q_{t,pos} = \int (q_{t,pos}) dt$, $Q_{t,neg} = \int (q_{t,neg}) dt$, $Q_{t,net} = Q_{t,pos} + Q_{t,neg}$



Overview of input parameters

Flow width	b	500 (m)	
Water depth (average value over tide and width)	h	15 (m)	
River discharge (negative in seaward direction)	Q	-500 (m ³ /s)	
Wave height	Hs	0 (m)	
Wave period	Tp	7 (s)	
Tidal peak velocity (landward is +; seaward is -)	Upeak	1 (m/s)	
Tidal asymmetry factor	f-asymmetry	1 (-)	
Tidal amplitude= 0.5xtidal range H (m)	0.5H	1 (m)	
Tidal period	T	43200 (s)	
Phase lead of horizontal tide to vertical tide (+ = lead)	Phi	0.5 (hours)	
Density gradient $d\rho/dx$ (maximum value of about 0.001)	$d\rho/dx$	0.001 (kg/m ³ /m)	
Coefficient residual density-induced flow (0.5 to 2; default 1) (smaller gamma gives larger effect)	gamma	1 (-)	
Dispersion coefficient at mouth (range of 500 to 1500)	Do	1000 (m ² /s)	
Location inside estuary (mouth x=0)	x	1000 (m)	
Salinity at mouth	So	25 (kg/m ³)	
Time at which flood velocity starts (Low water slack)	T-lws	1200 (sec)	see tidal plots
Back ground concentration mud (near the bed) during flood	c-flood	0 (kg/m ³)	
Back ground concentration mud (near the bed) during ebb	c-ebb	0 (kg/m ³)	
Sediment density	ρ_s	2650 (kg/m ³)	
Fluid density seawater = $1000 + 0.77 S_a$ -sea	ρ_{sea}	1025 (kg/m ³)	
Fluid viscosity	ν	0.000001 (m ² /s)	
Bed roughness for currents	$k_{s,c}$	0.1 (m)	
Bed roughness for waves	$k_{s,w}$	0.05 (m)	
Dry bulk density SAND fraction (incl. pores)	ρ -bulk sand	1600 (kg/m ³)	
Dry bulk density MUD fraction (incl. pores)	ρ -bulk	800 (kg/m ³)	
Percentage of MUD in bed (0 to 0.5): $P_{mud}+P_{gravel}+P_{sand}=1$	Pmud	0.2 (-)	
Percentage gravel (> 2 mm); (0 to 0.3)	Pgravel	0 (-)	
Percentage of SAND in bed (0 to 1)	Psand	0.8 (-)	
Single fraction			
Sand grain size d50 (see Cell B93)	d50	0.0002 (m)	
Sand grain size d90	d90	0.0005 (m)	
Suspended sediment size	dsus	0.00015 (m)	
Effective settling velocity of MUD (incl. flocculation)	w-s,mud	0.0005 (m/s)	
Multi fraction ($\sum P_{sand}$ should be equal to cellB40)			
Percentage of SAND fraction 0.062-0.125 mm	Psand1	0.1 (-)	
Percentage of SAND fraction 0.125-0.200 mm	Psand2	0.35 (-)	
Percentage of SAND fraction 0.200-0.300 mm	Psand3	0.3 (-)	Psand=
Percentage of SAND fraction 0.300-0.500 mm	Psand4	0.05 (-)	0.8
Percentage of SAND fraction 0.500-1.00 mm	Psand5	0 (-)	
Percentage of SAND fraction 1.00-2.00 mm	Psand6	0 (-)	
General parameters			
Reference level bed concentration	a	0.05 (m)	range=0.01-0.1 m
Time step	ΔT	300 (s)	
Calibration factor of SAND transport (formulae)		1 (-)	Default=1
Calibration factor. Ref. Concentration Susp. SAND (conc. profiles)		1 (-)	Default=1

Table 5.1 Model input data



5.7 Example computations

5.7.1 River flow over sand bed

The TSAND-model can also be used for river flow by setting the peak tidal velocity and the tidal amplitude of the water level to zero.

The model results have been compared to measured suspended transport rates in field conditions (Van Rijn 2007). The computed results of the single and multi-fraction methods are given in **Table 5.2** and **Figures 5.2** and **5.3**. The single fraction method requires input of the suspended sediment size (d_{sus}).

Figure 5.2 shows measured and computed suspended transport rates for sediment in the range of 0.1 to 0.2 mm (100 to 200 μm). The multi-fraction method yields values which are close to those of the single fraction method, if the suspended sediment size (d_{sus}) of the single fraction method is taken as $d_{sus}=0.85d_{50}$. The single fraction method yields values which are much smaller (factor 2) than those of the multi-fraction method if the suspended sediment size (d_{sus}) of the single fraction method is taken equal to the d_{50} . Both methods (single fraction and multi fraction) underpredict considerably for velocities < 1 m/s.

$d_{50}=0.175$ mm (175 μm), $d_{90}=0.5$ mm fraction 1 = 0.063-0.125mm; percentage= 0.25 fraction 2 = 0.125-0.2 mm; percentage = 0.50 fraction 3 = 0.2-0.3 mm; percentage= 0.2 fraction 4 = 0.3-0.5 mm; percentage= 0.05 fraction 5 = 0.5-1 mm; percentage= 0 fraction 6 = 1-2 mm; percentage= 0 water depth= 6 m					$d_{50}=0.285$ mm (285 μm), $d_{90}=0.9$ mm fraction 1 = 0.063-0.125mm; percentage= 0.1 fraction 2 = 0.125-0.2 mm; percentage = 0.2 fraction 3 = 0.2-0.3 mm; percentage= 0.35 fraction 4 = 0.3-0.5 mm; percentage= 0.3 fraction 5 = 0.5-1 mm; percentage= 0.05 fraction 6 = 1-2 mm; percentage= 0 water depth= 6 m				
Depth-mean velocity (m/s)	Bed roughness (m)	Suspended transport single fraction $d_{sus}=0.15$ mm (kg/m/s)	Suspended transport single fraction $d_{sus}=0.175$ mm (kg/m/s)	Suspended transport multi fraction (kg/m/s)	Depth-mean velocity (m/s)	Bed roughness (m)	Suspended transport single fraction $d_{sus}=0.2$ mm (kg/m/s)	Suspended transport single fraction $d_{sus}=0.285$ mm (kg/m/s)	Suspended transport multi fraction (kg/m/s)
0.4	0.1	0.00014	0.00095	0.0019	0.4	0.1	0.00026	0.00006	0.002
0.5	0.1	0.0044	0.0026	0.0075	0.5	0.1	0.0025	0.0012	0.0066
0.6	0.1	0.019	0.013	0.026	0.6	0.1	0.012	0.0052	0.02
0.8	0.1	0.16	0.11	0.21	0.8	0.1	0.12	0.041	0.14
1.0	0.05	0.51	0.36	0.66	1.0	0.1	0.41	0.174	0.48
1.2	0.03	1.32	0.91	1.6	1.2	0.08	1.06	0.52	1.2
1.4	0.02	2.9	2.0	3.5	1.4	0.06	2.3	1.24	2.5
1.6	0.01	5.3	3.6	6.2	1.6	0.04	4.4	2.35	4.6
1.8	0.005	9.0	4.9	10.2	1.8	0.03	7.7	4.0	7.8
2.0	0.001	12.6	8.5	14.0	2.0	0.02	12.5	6.3	12.5

Table 5.2 Computed suspended transport for river flow over sand bed

Figure 5.3 shows measured and computed suspended transport rates for sediment in the range of 0.2 to 0.4 mm (200 to 400 μm). The multi-fraction method yield values which are close to those of the single fraction method, if the suspended sediment size (d_{sus}) of the single fraction method is taken as $d_{sus}=0.7d_{50}$. The single fraction method yields values which are much smaller (factor 2) than those of the multi-fraction method if the suspended sediment size of the single fraction method is taken equal to the d_{50} . The results of the multi-fraction method are in good agreement with the measured values. The multi-fraction method slightly



overpredicts for very large velocities >1.5 m/s. The single fraction method underpredicts substantially for small velocities close to initiation of motion.

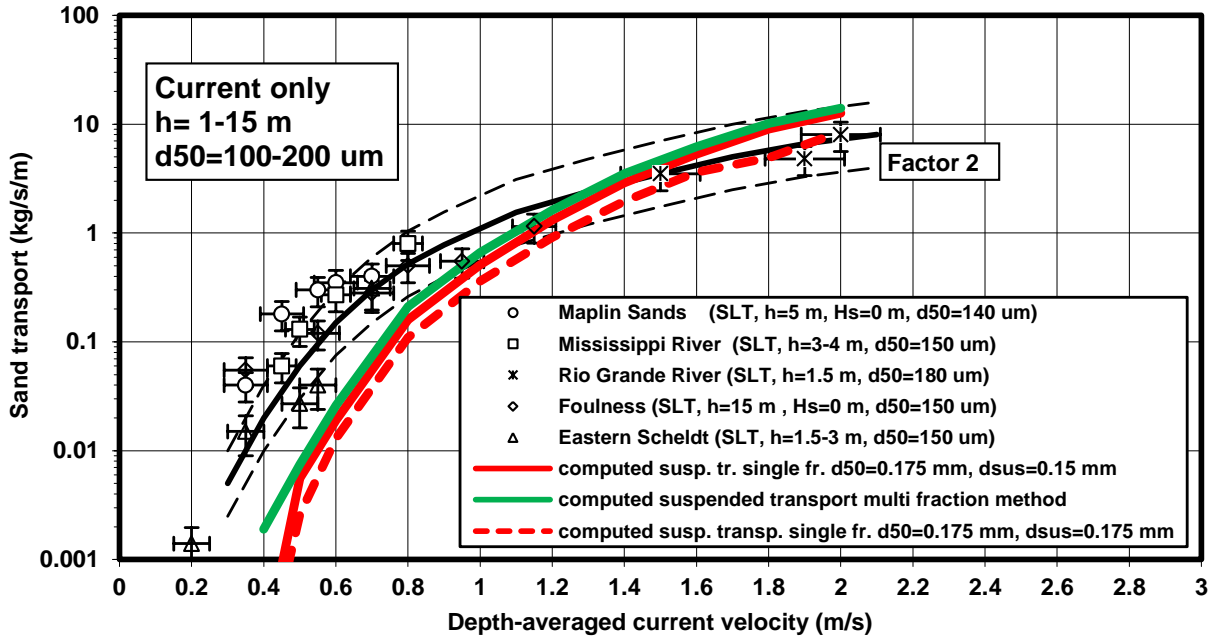


Figure 5.2 Measured and computed suspended transport; 100-200 μm

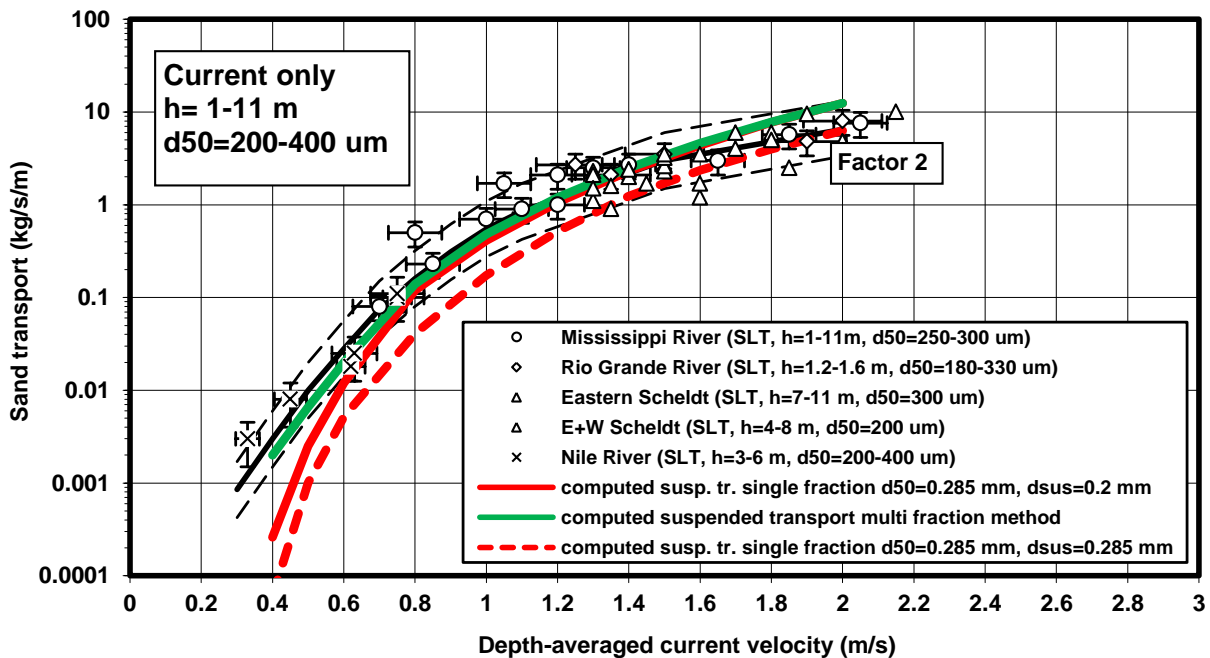


Figure 5.3 Measured and computed suspended transport; 200-400 μm



5.7.2 Tidal flow over sand-mud bed

Three example computations are presented. The input data are given in **Table 5.2**.

The results of example computation **Case 1** are shown in **Figures 5.4** and **5.5**.

The effect of the salinity gradient on the velocity profiles at peak flood and peak ebb flow can be clearly seen in **Figure 5.5**.

The time lag effect of the suspended sand concentrations is about 15 min, see **Figure 5.3**. The time lag effect reduces to almost zero for sediment of about 0.25 mm (fall velocity of about 0.025 m/s) resulting in quasi-steady equilibrium transport. The mud concentration profile is much more uniform than the sand concentration profile.

Input parameters	Input values Case 1	Input values Case 2	Input values Case 3
Flow width b (m)	500	500	500
River discharge Q (m ³ /s)	-500	-500	-1500
Tide and width-averaged water depth h _o (m)	15	15	15
Tidal amplitude $\eta_o = 0.5H$ (H=tidal range), (m)	1	1	1
Tidal peak velocity U _{max} (m/s)	1	1	1
Phase between horizontal and vertical tide (hours)	0.5	0.5	0.5
Tidal asymmetry f _a (-)	1	1.1	1.1
Tidal period T (s)	43200	43200	43200
Salinity-related density gradient dρ/dx (kg/m ³ per m)	0.001	0.001	0.001
Coefficient salinity-related residual flow (-)	1	1	1
Dispersion at mouth for salinity (range 500 to 1500 m ² /s)	1000	1000	1000
Location inside estuary with respect to mouth x	1000	1000	1000
Salinity at mouth S _o (kg/m ₃)	25	25	25
Time at which low water slack occurs T _{LWS} (s)	1200	1200	1200
Significant wave height H _s (m)	0	0	0
Peak wave period T _p (s)	0	0	0
Percentage sand and mud	0.8; 0.2	0.8; 0.2	0.8; 0.2
Single fraction method: sand diameters d ₅₀ , d ₉₀ , d _{sus} (m)	0.0002; 0.0005; 0.00015	0.0002; 0.0005 0.00015	0.0002; 0.0005; 0.00015
Multifraction method fraction 1 = 0.063-0.125mm, fraction 2 = 0.125-0.2 mm, fraction 3 = 0.2-0.3 mm, fraction 4 = 0.3-0.5 mm, fraction 5 = 0.5-1 mm, fraction 6 = 1-2 mm	0.10 0.35 0.30 0.05 0 0	0.10 0.35 0.30 0.05 0 0	0.10 0.35 0.30 0.05 0 0
Fall velocity mud w _{s,mud} (m/s)	0.0005	0.0005	0.0005
Dry bulk density of sand and mud ρ _{dry} (kg/m ³)	1600; 800	1600; 800	1600; 800
Bed roughness current k _{s,c} and waves k _{s,w} (m)	0.10; 0.05	0.10; 0.05	0.10; 0.05
Reference level concentration profile a (m)	0.05	0.05	0.05
Sediment density ρ _s (kg/m ³)	2650	2650	2650
fresh water fluid density ρ _{fresh} (kg/m ³)	1000	1000	1000
Sea water density ρ _{sea} (kg/m ³)	1025	1025	1025
Kinematic viscosity coefficient ν (m ² /s)	0.000001	0.000001	0.000001
Time step Δt (s)	300	300	300

Table 5.2 Input data

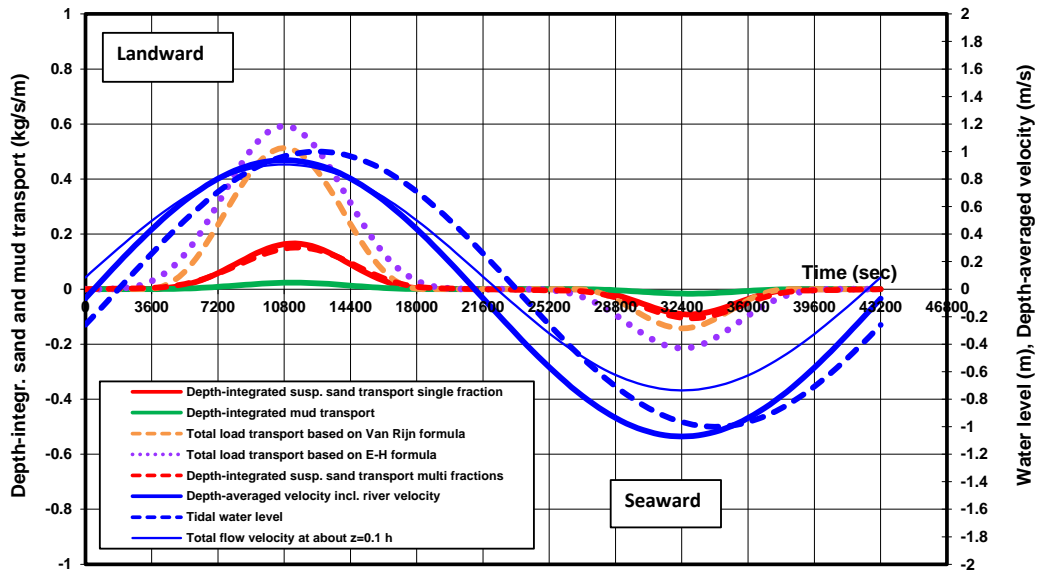


Figure 5.4 Suspended sand transport as function of time in tidal flow; Case 1

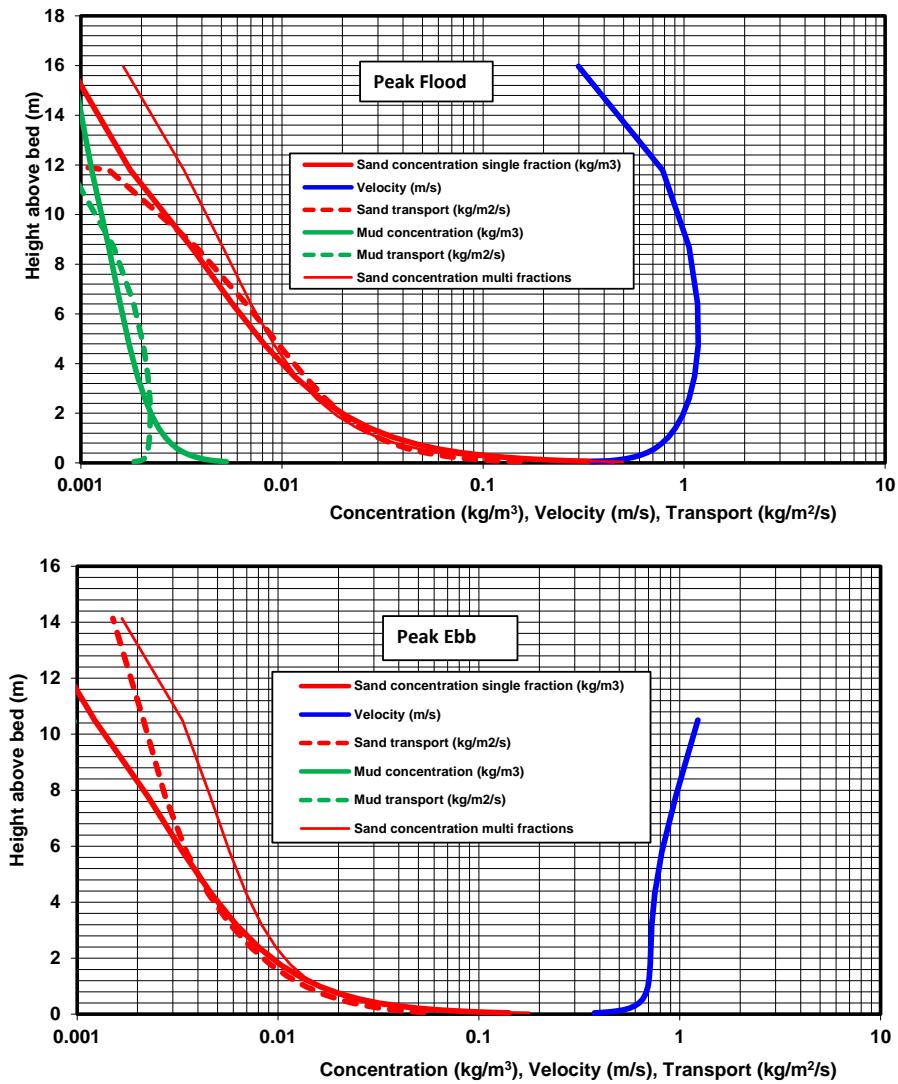


Figure 5.5 Vertical profiles of suspended sand concentration, velocity and transport; Case 1



Tide- integrated and width-integrated sediment transport rates are given in **Table 5.3**.

- Case 1 with symmetrical tide and low freshwater discharge:** sand and mud transport due to the salinity gradient effect is landward:
- Case 2 with asymmetrical tide and low freshwater discharge:** landward sand and mud transport increases by about factor 2 due tidal asymmetry effect in addition to the salinity gradient effect.
- Case 3 with asymmetrical tide and high freshwater discharge:** landward sand transport based on formula-approach decreases significantly; seaward sand and mud transport based on the concentration profile approach.

Case 2 yields a net annual landward sand transport of about $730 \times 850 = 0.6$ million tons $\cong 0.4$ million m^3 (import) in a channel of width= 500 m assuming 730 tides per year and bulk density of 1.6 tons/ m^3 .

Case 3 yields a net annual seaward sand transport of about $730 \times -200 = -0.15$ million tons $\cong -0.1$ million m^3 (export).

Case	Type of approach	Flood-integrated transport (ton/flood tide)	Ebb-integrated transport (ton/ebb tide)	Net tide-integrated transport (ton/tide) += landward -= seaward
1 Sym. Tide Q=-500 m ³ /s	Engelund-Hansen sand transport formula	2300	-740	1560
	Van Rijn sand transport formula	1780	-400	1380
	Van Rijn sand concentration profiles (single fr.)	660	-300	360
	Van Rijn sand concentration profiles (multi fr.)	890	-520	370
	Van Rijn mud concentration profiles	80	-50	30
2 Asym. Tide Q=-500 m ³ /s	Engelund-Hansen sand transport formula	3180	-480	2700
	Van Rijn sand transport formula	2670	-170	2500
	Van Rijn sand concentration profiles (single fr.)	1000	-140	860
	Van Rijn sand concentration profiles (multi fr.)	1210	-340	870
	Van Rijn mud concentration profiles	125	-25	100
3 Asym. Tide Q=-1500 m ³ /s	Engelund-Hansen sand transport formula	1580	-1270	310
	Van Rijn sand transport formula	1170	-800	370
	Van Rijn sand concentration profiles (single fr.)	430	-590	-160
	Van Rijn sand concentration profiles (multi fr.)	630	-900	-270
	Van Rijn mud concentration profiles	55	-95	-40

Table 5.3 Tide- and width-integrated sediment transport rates



6. Time-dependent 2DV sediment transport model for tidal flow (SUSTIM2DV.xls)

6.1 General

The numerical SUSTIM-model solves the time dependent 3D advection-diffusion equation for suspended sediment concentrations. The 3D advection-diffusion equation can be solved when the following parameters are known: 1) flow field (u, v, w); 2) sediment mixing coefficients ($\varepsilon_{s,x}, \varepsilon_{s,y}, \varepsilon_{s,z}$); 3) settling velocity (w_s) and 4) sediment concentrations at all boundaries and at initial time. The 2DV-model is derived from the 3D-model by setting the lateral components to zero. The SUSTIM-model can be used for sandy and muddy environments.

The sediment mixing coefficients are related to basic current and wave parameters. The settling velocity depends on the sediment concentration to include the effects of flocculation and hindered settling in mud suspensions.

The bed-boundary condition (reference concentration) is represented by an empirical equation specifying the near-bed concentration as function of the local bed-shear stress.

The velocities and mud concentrations are computed as a function of z and t ; z =height above bed and t =time . The grid points over the depth (25 to 100 points) are distributed according to an exponential function over the water column. The bed is defined at $z=0$. The grid points are distributed between $z=0$ and the water surface at each time.

The effect of the number of vertical grid points ($NZ=10, 25, 50$ and 100) on the computed sand concentration profile was studied for a channel with a constant depth of $h=10$ m and steady flow of 1.35 m/s (no tide). Other parameters are: sand $d_{50}=0.2$ mm; $w_s=0.015$ m/s, $k_s=0.03$ m $z_a=0.05$ m, $\beta=1$. The bed concentration for sand is set to 5 kg/m³ (applied at $z=0$ m). The computed sand concentration profiles for $NZ=10, 25, 50$ and 100 are shown in **Figure 6.1**. The analytical Rouse concentration profile $c=c_a [((h-z)/z)(a/(h-a))]^{ws/(\beta k_s u_*^*)}$ based on a parabolic mixing coefficient distribution is also shown. The computed values of the numerical SUSTIM2DV-model for $NZ=50$ and 100 are in good agreement with the analytical values in the lower half of the depth. The analytical concentrations are lower in the upper half due to parabolic mixing coefficient distribution, whereas a constant value is used in the numerical model. At least, 25 to 50 grid points are required for accurate results.

A detailed description of the SUSTIM2DV-model is given by Van Rijn (2023).

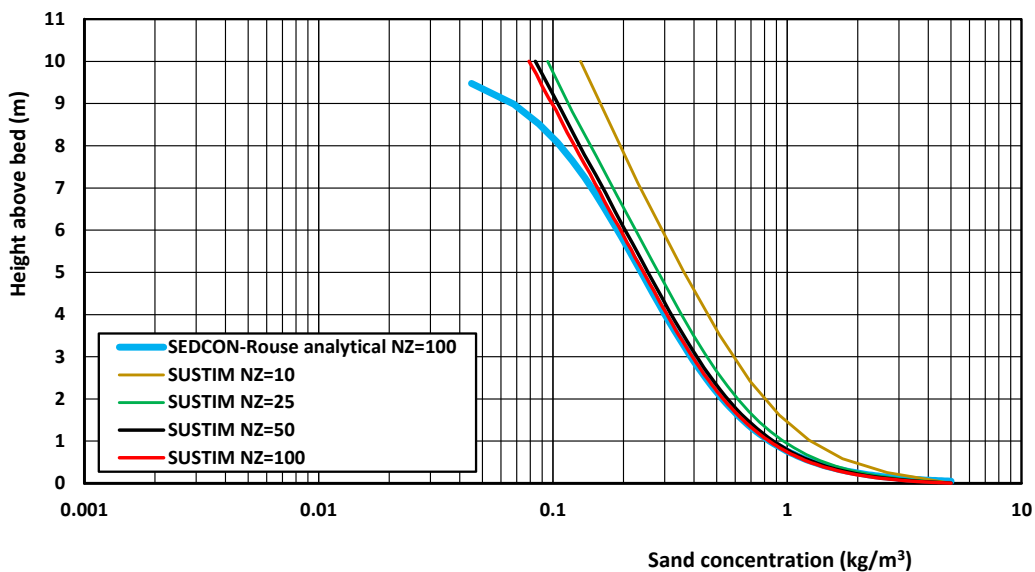


Figure 6.1 Effect of vertical grid points on computed sediment concentration profile in steady current



6.2 Flow field

The SUSTIM2DV-model can be used for conditions with a constant water depth or a varying water depth.

$$\text{Tidal variation: } \eta_t = \eta_{\max} \sin(\omega t) \quad (6.1)$$

$$\text{Water depth at boundary: } h_{o,t} = h_{\text{MSL},o} + \eta_t \quad (6.2a)$$

$$\text{Current at boundary: } u_{o,t} = u_{mo} + u_{\max o} \sin(\omega t + \varphi) \quad (6.2b)$$

$$\text{Current along traject: } u_{x,t} = h_{o,t} u_{o,t} / h_{x,t} \quad (6.3)$$

u_o = depth-averaged current velocity at $x=0$, u_{mo} = constant depth-averaged velocity at $x=0$ (input), $u_{\max o}$ = depth-averaged amplitude of current velocity at $x=0$ (input), $h_{\text{MSL},o}$ = depth between bottom and mean sea level at $x=0$, η_{\max} = tidal amplitude, h_o = water depth at inflow boundary (water depth outside channel), h_x = local water depth (bottom to surface), $\omega = 2\pi/T$; T = tidal period, x = longitudinal coordinate.

Equation (6.3) is used to determine the current velocity over a varying bed profile (pipeline trench, shipping channel, sediment mound). Additional equations are implemented in the model to represent oblique flow over a varying bed profile. Herein, only cases with flow normal to a trench, pit or channel are simulated.

The vertical distribution of the velocity at coordinate x is assumed to be logarithmic and is described as:

$$u_{z,t} = (z/\delta_{fm}) u_{b,t} \quad \text{for } z \leq \delta_{fm} \quad (6.4a)$$

$$u_{z,t} = u_t [(-1 + \ln(h_x/z_o))]^{-1} \ln(z/z_o) \quad \text{for } z > \delta_{fm} \quad (6.4b)$$

$$u_{b,t} = u_t [(-1 + \ln(h_x/z_o))]^{-1} \ln(\delta_{fm}/z_o) \quad (6.4c)$$

with: $u_{b,t}$ = near-bed velocity vector at level $z = \delta_{fm}$ at time t , u_t = depth-averaged current velocity
 δ_{fm} = thickness of high-concentration fluid mud layer (input value), z = level above bed (m), h_x = water depth at time t , $z_o = 0.033k_{s,c}$ = zero-velocity level, $k_{s,c}$ = current-related bed roughness (wave-current interaction is neglected).

The velocity inside the fluid mud layer (if present) is assumed to be linear, see Equation (6.4a).

The vertical fluid velocity (w) follows from the continuity equation for the fluid ($\partial u/\partial x + \partial w/\partial z = 0$).

6.3 Basic sediment equations

The time dependent 3D advection-diffusion equation reads, as:

$$\partial c/\partial t + \partial(u c - \varepsilon_{s,x} \partial c/\partial x)/\partial x + \partial(v c - \varepsilon_{s,y} \partial c/\partial y)/\partial y + \partial((w - w_s) c - \varepsilon_{s,z} \partial c/\partial z)/\partial z = 0 \quad (6.5)$$

with:

c = sediment concentration (volume), u, v, w = fluid velocities in x, y and z direction, w_s = settling velocity,

$\varepsilon_{s,x}, \varepsilon_{s,y}, \varepsilon_{s,z}$ = sediment mixing coefficients in x, y and z direction,

x = longitudinal coordinate, y = lateral coordinate (set to 1 m), z = vertical coordinate.

The 2DV advection-diffusion equation for uniform flow in longitudinal direction reads as:

$$\partial c/\partial t - \partial c w_s/\partial z - \partial(\varepsilon_s \partial c/\partial z)/\partial z = 0 \quad (6.6)$$

with:

c = concentration (volume), w_s = settling velocity of suspended material, ε_s = sediment mixing coefficient.

In the case of a steady current ($\partial c/\partial t = 0$; $u = \text{constant}$), Equation (6.6) gives the equilibrium concentration profile, as follows:

$$c w_s + \varepsilon_s \partial c/\partial z = 0 \quad (6.7)$$



As the settling velocity and the sediment mixing coefficient are both dependent on the concentration, Equation (6.7) can only be solved numerically and is used at the inflow boundary. The sand and mud concentrations at initial time (t=0) are set to zero (c=0).

The bed-shear stresses at time t due to currents and waves are represented as:

$$\tau_{b,c} = \rho_w \kappa^2 u_b^2 / [\ln(30z_b/k_{s,c})]^2 \quad (6.8a)$$

$$\tau_{b,c} = 0.125 \rho_w \alpha_w f_c (u_c)^2 \quad (6.8b)$$

$$\tau_{b,w} = 0.25 \rho_w f_w (U_w)^2 \quad (6.9)$$

$$\tau_{b,cw} = \tau_{b,c} + \tau_{b,w} \quad (6.10)$$

with: $\tau_{b,c}$ =current-related bed-shear stress, $\tau_{b,w}$ =wave-related bed-shear stress,

$\tau_{b,cw}$ =bed-shear stress due to combined current and waves,

h=water depth, u_c = depth-averaged current velocity (m/s),

$U_w = (2\pi/T_p)A_w$ =peak orbital velocity (linear wave theory),

A_w = peak orbital excursion, T_p = peak wave period,

$\alpha_w = [\ln(30\delta_b/k_a)/\ln(30\delta_b/k_{s,c})]^2 [(-1+\ln(30h/k_{s,c})) / (-1+\ln(30h/k_a))]^2$ =wave-related coefficient ($0 < \alpha_w \leq 1$),

$f_w = \exp(-6+5.2(A_w/k_{s,w})^{-0.19})$ = wave-related friction coefficient,

$f_c = 0.24 / (\log(12h/k_{s,c}))^2$ = current-related friction coefficient,

h= water depth, δ_b =wave-related mixing layer near bed,

H_s = significant wave height, T_p = peak wave period,

$k_{s,c}$ = current-related roughness, $k_{s,w}$ = wave-related roughness,

k_a = apparent bed roughness for current (range 1 to 5 $k_{s,c}$),

ρ_s = sediment density (input value), ρ_w = fluid density (input value).

The effective bed-shear stresses at time t for sediment transport are represented as:

$$\tau_{b,c}' = \mu_c \tau_{b,c} \quad (6.11)$$

$$\tau_{b,w}' = \mu_w \tau_{b,w} \quad (6.12)$$

with: μ_c = current-related efficiency factor, μ_w = wave-related efficiency factor.

Sand: the reference concentration c_a is represented, as:

$$c_{a,sand} = 0.015 (1-p_{mud}) (d_{50}/a) [(\tau'_{b,cw} - \tau_{b,cr,o}) / \tau_{b,cr,o}]^{1.5} (D^*)^{0.3} \quad (6.13)$$

with: d_{50} = median particle diameter, $D^* = d_{50}[(s-1)g/v^2]^{0.333}$ = dimensionless particle parameter,

$\tau_{b,cr} = (1+p_{mud})^2 \tau_{b,cr,o}$ = critical bed-shear stress of sand mixed with some mud,

$\tau_{b,cr,o}$ = critical bed-shear stress of sand based on d_{50} (Shields' curve).

$\tau'_{b,cw} = \mu_c \tau_{b,c} + \mu_w \tau_{b,w}$ = effective bed-shear stress due to current and waves,

$\mu_c = f_c' / f_c$ = current-related efficiency factor,

$f_c = 0.24 / [\log(12h/k_{s,c})]^2$ = current-related friction coefficient,

$f_c' = 0.24 / [\log(12h/(3d_{90}))]^2$ = grain-related friction coefficient, d_{90} = grain size,

$\mu_w = 0.7/D^*$ = wave-related efficiency factor ($\mu_{w,min}=0.14$, $\mu_{w,max}=0.35$ based on d_{50}),

$s = \rho_s / \rho_w$ = relative density, v = kinematic viscosity coefficient, ρ_s = sediment density (input value),

a = reference level above the bed, p_{mud} = fraction of mud (<0.062 mm) of top layer of bed.

Mud: the boundary condition at the bed is represented by the reference bed concentration $c_{a,mud}$, as follows:

$$c_{a,mud} = \alpha_{mud} [\tau'_{b,cw} - \tau_{b,cr,e}] / \tau_{b,cr,e} \quad \text{for } du/dt > 0 \text{ (accelerating tidal flow)} \quad (6.14a)$$

$$dc_{a,mud}/dz = 0 \quad \text{for } du/dt < 0 \text{ (decelerating tidal flow; } c_{a,t} < c_{a+1, t-\Delta t}) \quad (6.14b)$$

with: α_{mud} = erosion coefficient (input value), p_{mud} = fraction of mud of top layer of bed (input value),



$\tau_{b,cr,e}$ = critical bed-shear stress for erosion (input value),
 $\tau_b/\rho = \mu_c \tau_{b,c} + \mu_w \tau_{b,w}$ = effective bed-shear stress due to current and waves,
 $\mu_c = f_c / f_{c,c}$ = current-related efficiency factor=1 for mud, μ_w = wave-related efficiency factor =0.35 for mud.
 Equation (6.14b) means no upward flux of mud from the bed into suspension during decelerating flow;
 sediment settles on the bed at rate $c_{a,mud} w_s$.

The settling velocity is described, as:

Sand: the settling velocity of sand is assumed to be constant.

Mud: the mud settling velocity is concentration-dependent and represented as:

$$w_{mud} = \exp[\alpha_1 \ln(c) + \alpha_2 - \alpha_3]; \quad \text{for flocculation range } c \leq 0.0025 \quad (6.15a)$$

$$\alpha_1 = 0.182 \ln(w_{mud,max}/w_{mud,min})$$

$$\alpha_2 = 2.09 \ln(w_{mud,max})$$

$$\alpha_3 = 1.09 \ln(w_{mud,min})$$

$$w_{mud} = w_{mud,max}(1-c)^4 \quad \text{for hindered settling range } c > 0.0025 \quad (6.15b)$$

with:

$w_{mud,max}$ = maximum settling velocity at $c=0.0025$ (input value),

$w_{mud,min}$ =minimum settling velocity at $c=0.00001$ (input value).

The settling velocity at height z is determined by using the concentration values at $t-\Delta t$.

Equation (6.15) with $w_{mud,max}=0.001$ m/s and $w_{mud,min}=0.0001$ m/s, is shown in **Figure 6.2**.

Using a concentration-dependent settling velocity, the transport of mud < 32 μm can be represented by one single fraction.

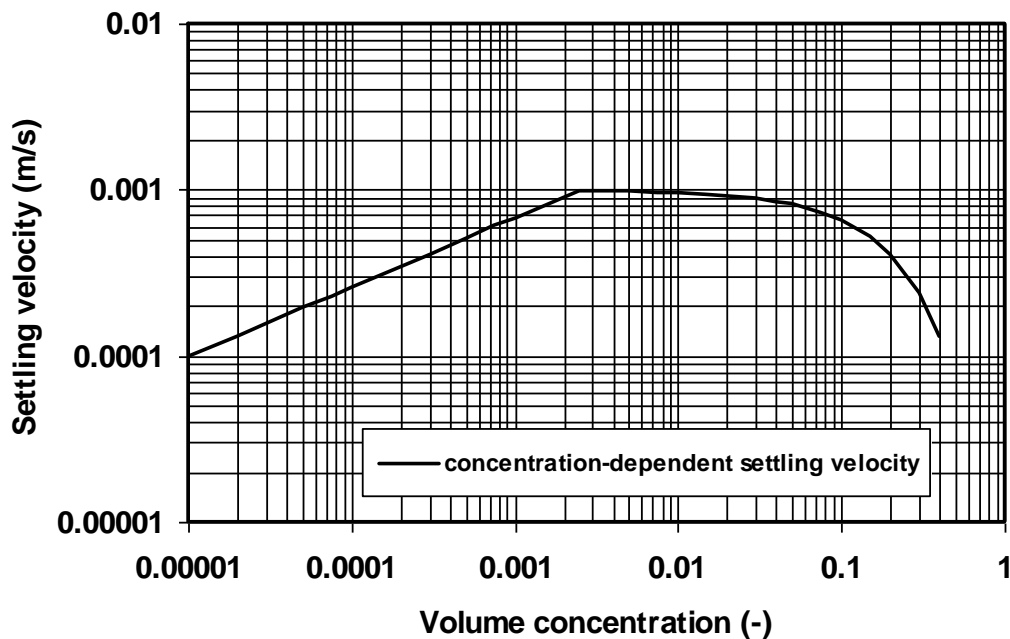


Figure 6.2 Settling velocity as function of volume concentration; flocculation range for $c < 0.0025$ and hindered settling range for $c > 0.0025$; $w_{mud,max}=0.001$ m/s (1 mm/s), $w_{mud,min}=0.0001$ m/s (0.1 mm/s)



For combined steady and oscillatory flow, the sediment mixing coefficient is modelled as:

$$\varepsilon_{s,cw} = [(\varepsilon_{s,c})^2 + (\varepsilon_{s,w})^2]^{0.5} \quad (6.16)$$

in which: $\varepsilon_{s,w}$ = wave-related mixing coefficient (m^2/s), $\varepsilon_{s,c}$ = current-related mixing coefficient (m^2/s).

Sand: the vertical distribution of the current-related mixing is parabolic-constant (**Figure 6.3**) over the depth:

$$\varepsilon_{s,c} = \varepsilon_{s,c,max} - \varepsilon_{s,c,max}(1-2z/h)^2 \quad \text{for } z/h < 0.5 \quad (6.17a)$$

$$\varepsilon_{s,c} = \varepsilon_{s,c,max} = 0.25 \beta \kappa u_{*,c} h = 0.1 \beta u_{*,c} h \quad \text{for } z/h \geq 0.5 \quad (6.17b)$$

with: β = ratio of sediment and fluid mixing coefficient (input parameter, default=1, range 0.5-1.5), $\kappa=0.4$ = constant of Von Karmann, $u_{*,c} = (\tau_{b,c}/\rho_w)^{0.5}$ = current-related bed-shear velocity, h = water depth.

The vertical distribution of the wave-related mixing is linear-constant (**Figure 6.3**) over the depth:

$$\varepsilon_{s,w} = \varepsilon_{s,w,bed} \quad \text{for } z \leq \delta_b \quad (6.18a)$$

$$\varepsilon_{s,w} = [\varepsilon_{s,w,bed} + (\varepsilon_{s,w,max} - \varepsilon_{s,w,b}) (z - \delta_b) / (0.5h - \delta_b)] \quad \text{for } \delta_b < z < 0.5h \quad (6.18b)$$

$$\varepsilon_{s,w} = \varepsilon_{s,w,max} \quad \text{for } z \geq 0.5h \quad (6.18c)$$

$$\varepsilon_{s,w,bed} = 0.018 \gamma_4 \delta_b U_w \quad (6.18d)$$

$$\varepsilon_{s,w,max} = 0.035 \gamma_3 h H_s / T_p \quad \text{with } \varepsilon_{s,w,max} \leq 0.05 \text{ m}^2/\text{s}. \quad (6.18e)$$

with:

$\varepsilon_{s,w,bed}$ = wave-related sediment mixing coefficient near the bed,

$\varepsilon_{s,w,max}$ = maximum wave-related sediment mixing coefficient at mid-depth ($z/h=0.5$),

δ_b = wave-related mixing layer thickness near the bed, γ_3, γ_4 = scaling calibration coefficients (range 0.25-1).

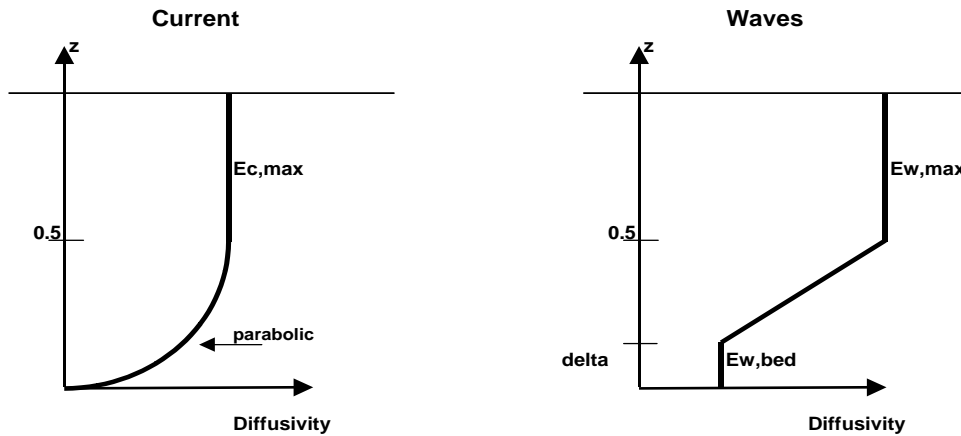


Figure 6.3 Vertical distribution of mixing coefficients

Mud: wave-related sediment mixing coefficient for muddy conditions is represented by Equation (6.18); current-related sediment mixing coefficient distribution in the presence of fluid mud (if present) near the bed is represented by:

$$\varepsilon_s = \phi_d \varepsilon_{bfm} \quad \text{for } z \leq \delta_{fm} \quad (6.19a)$$

$$\varepsilon_s = \phi_d [\varepsilon_{b,fm} + (\varepsilon_{max} - \varepsilon_{bfm}) (z - \delta_{fm}) / (0.5h - \delta_{fm})]^n \quad \text{for } \delta_{fm} < z < 0.5h \quad (6.19b)$$

$$\varepsilon_s = \phi_d [(h-z)/(0.5h)]^n \varepsilon_{max} \quad \text{for } z \geq 0.5h \quad (6.19c)$$

$$\varepsilon_{max} = \gamma_1 u_{*,c} h$$

$$\varepsilon_{bfm} = \gamma_2 \varepsilon_{max}$$

$$\varepsilon_{min} = 0.001 \text{ m}^2/\text{s}$$



with:

δ_{fm} = thickness of fluid mud layer (input value), ε_{bfm} = sediment mixing coefficient in fluid mud layer, ε_{max} = maximum sediment mixing coefficient at mid-depth ($z/h=0.5$), ε_{min} = 0.001 m²/s = minimum value at slack tide conditions, h = water depth, $u_{*,c} = (\tau_{b,c}/\rho_w)^{0.5}$ = current-related bed-shear stress of current velocity vector,

γ_1 = scaling calibration coefficient (range=0.01-0.1; $\gamma_1 = 0.1$ gives Equation 6.17b),

γ_2 = scaling calibration coefficient (range=0.05-0.5),

n = exponent (input parameter; linear for $n=1$; approximately parabolic for $n \leq 0.5$),

ϕ_d = turbulence damping coefficient (function of Richardson number),

$Ri = [-(g/\rho)][d\rho/dz]/[(du/dz)^2] = [-(\rho_s - \rho_w)g/((\rho_w + (\rho_s - \rho_w)c)][dc/dz]/[(du/dz)^2]$ = Richardson number (salinity and temperature effects on the vertical density gradient are neglected),

ρ = fluid-sediment mixture density = $\rho_s c + (1-c)\rho_w$, c = volume concentration.

The damping function is expressed as:

$$\phi_d = (1 + \alpha_d 2Ri^{0.5})^{-1} \quad (6.20)$$

with: α_d = calibration coefficient (default=1; in range of 0 to 2), Ri = Richardson number (-).

Figure 6.4 shows the vertical distribution of the current-related mixing coefficient for mud with $n=0.5$, 1 and 2. The other parameters are: water depth is $h=10$ m; δ_{fm} = fluid mud layer = 1 m; ε_{max} = 0.05 m²/s; ε_{bfm} = 0.01 m²/s. For $n=1$, the mixing coefficient is linear between the fluid mud layer and the water surface; increasing from the top of the fluid mud layer up to mid-depth and decreasing from mid-depth to water surface. For $n=0.5$, the distribution is almost parabolic, as used for sand (Equation 6.17a) resulting in higher concentrations (lower concentrations for $n=2$).

Using a parabolic mixing coefficient distribution, the well-known Rouse-concentration profile is obtained.

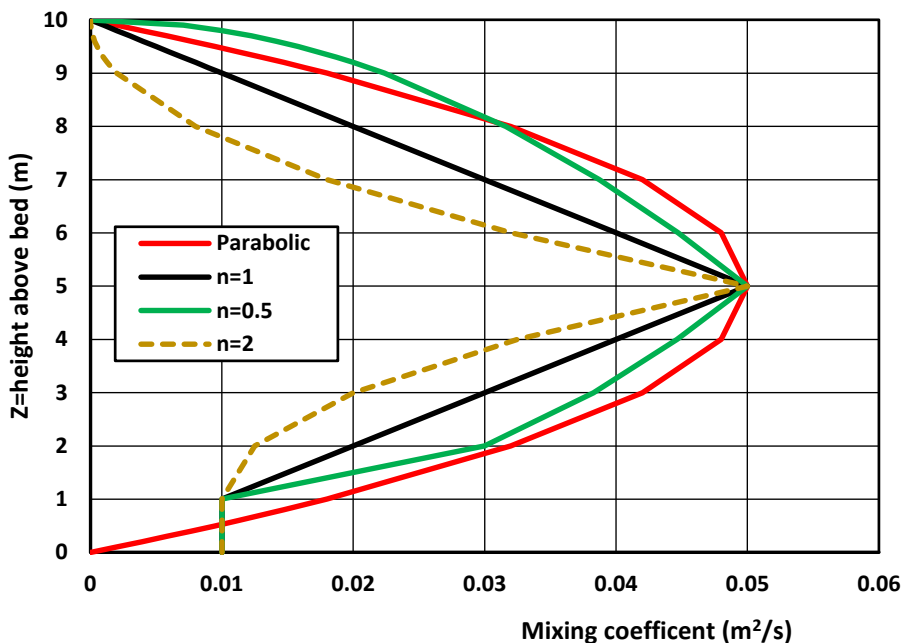


Figure 6.4 Vertical distribution of current-related mixing coefficient for mud; water depth=10 m



The depth-integrated sand or mud transport rate (kg/m/s) at each time t is computed as:

$$q_{s,sand,x} = a \int_a^h (u_x C - \varepsilon_{s,x} \partial C / \partial x) dz; \quad (6.21a)$$

$$q_{s,mud,x} = a \int_a^h (u_x C - \varepsilon_{s,x} \partial C / \partial x) dz; \quad (6.21b)$$

The bed load transport (kg/m/s) is computed as:

$$q_{b,sand,x} = 0.5 \gamma_b \rho_s d_{50} / D^{0.3} u'^*_c [\tau'_{b,cw} - \tau_{b,cr} / \tau_{b,cr}] \quad (6.22)$$

with: γ_b =scaling coefficient, u'^*_c =grain-friction-related bed-shear velocity due to current (m/s), $\tau'_{b,cw}$ =effective bed-shear stress due to current and waves.

The bed load transport (kg/m/s) of mud is computed as:

$$q_{b,mud,x} = c_a a u_b \quad (6.23)$$

with: c_a = bed reference concentration (kg/m³), a =reference level of bed concentration (m), u_b = near-bed velocity (m/s).

The bed level is computed from the sediment continuity equation (sources and sinks are neglected), as follows:

$$dz_b/dt + \gamma d(q_{b,x} + q_{s,x})/dx = 0 \quad (6.24)$$

with; z_b =bed level (m) to a datum at location x and at time t ; $q_{b,x} + q_{s,x}$ =bed load transport plus suspended load transport (kg/m/s); $\gamma = 1/\rho_{dry}$, ρ_{dry} =dry bulk density of bed (input value, kg/m³).

6.4 Modelling of sand concentrations, transport and bed level changes

Two cases are considered: 1) Sand concentration profiles in currents and waves; and 2) Sand transport in tidal channel, Eastern Scheldt, The Netherlands.

6.4.1 Case 1: Sand concentration profiles in currents and waves

To get a better understanding of the types of sand concentration profiles generated at a sandy bed ($d_{50}=0.2$ mm, $d_{90}=0.5$ mm) in conditions with currents and/or waves, the SUSTIM2DV-model (with 50 grid points over the depth of 10 m; time step=4 s) is used to compute the sand concentration profiles for:

- currents alone (depth-averaged maximum velocity $u=1.35$ m/s at $t=3$ hours of tidal cycle),
- wave alone (significant wave height $H_s=3$ m ; peak wave period $T_p=10$ s) and
- combined current and wave conditions in a water depth of 10 m (to MSL).

The settling velocity of suspended sand is set to $w_s=0.015$ m/s. The bed roughness is set to $k_{s,c}=k_{s,w}=0.03$ m. The tidal water level amplitude is 1 m. The tidal period is 12 hours. The scaling coefficient of the reference concentration at the bed is set to 1 (default). The scaling coefficients of the mixing coefficients are set to $\gamma_3=0.25$ and $\gamma_4=1$.

Figure 6.5 shows the computed sand concentration profiles. The sand concentrations for currents alone have the typical Rouse-type curve over the depth. The sand concentrations for waves alone are typically rather steep with high concentrations in the near-bed region ($z < 0.1$ h) and much lower concentrations higher up in the water column because the mixing effect of waves is less strong in the upper part of the depth. The sand concentrations for combined currents and waves are much higher than for currents alone or waves alone.

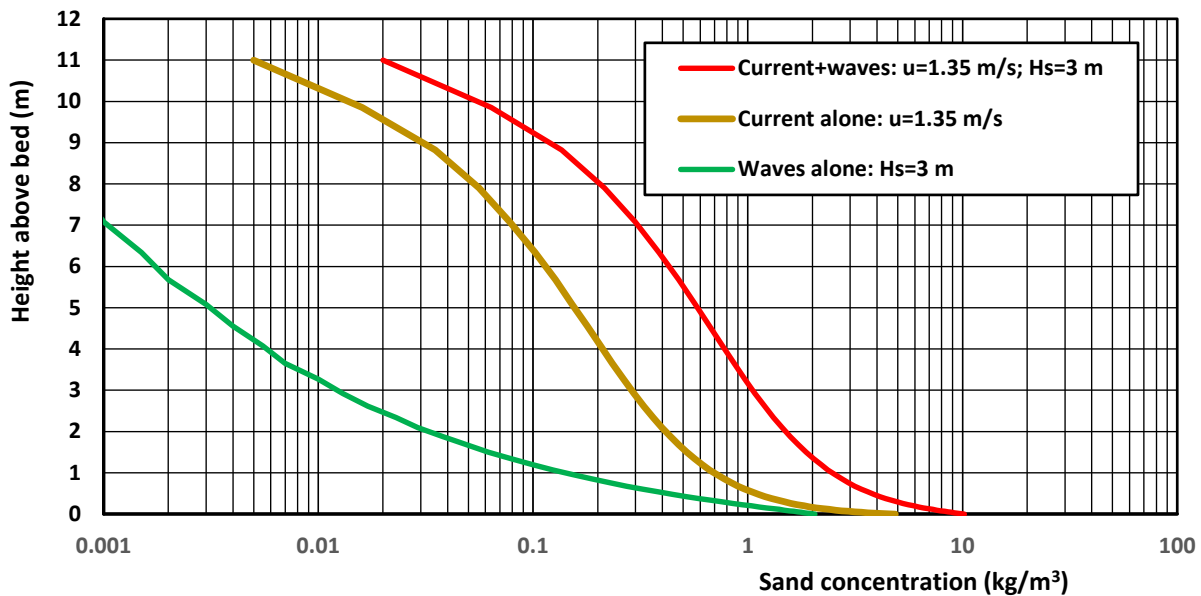


Figure 6.5 Computed sand concentrations for currents alone, waves alone and combined currents plus waves at $t=3$ hrs (maximum flow).

6.4.2 Case 2: Sand transport in tidal channel, Eastern Scheldt, The Netherlands

To demonstrate that the SUSTIM2DV-model can produce realistic sand concentrations and transport rates in field conditions, the model results are compared to measured sand transport values in a sandy tidal channel. In April 1987, detailed sand concentration and transport measurements were performed in a tidal channel of the Eastern Scheldt estuary in the southwest part of The Netherlands (Krammer channel, Station 2, 8 April 1987). The water depths were in the range of 7 to 8 m. The bed material was sand with $d_{50}=0.3$ mm and $d_{90}=0.6$ mm. The maximum flow velocity was up to 1.8 m/s. Flow velocity and sand concentrations were measured using an acoustic sand transport meter at 0.2 m and at 1 m above the bed, at mid-depth and at 2 m below the water surface. Additionally, sand concentrations were measured at 0.05, 0.1 and 0.2 m above the bed using a pump system. Based on the data, the depth-integrated sand transport was calculated (inaccuracy of about 30%). Settling tests with the suspended sand samples showed values in the range of 0.02 to 0.036 m/s. The basic input data are: water depth: $h=6$ to 8 m to MSL; tidal current with tidal period of 12 hours; maximum depth-averaged current: $u_{c,peak}=1.8$ m/s; no phase shift between water levels and current velocities; sand bed with $d_{50}=0.3$ mm; $d_{90}=0.6$ mm; bed roughness $k_{s,c}=k_{s,w}=k_a=0.2$ m derived from measured velocity profiles; a =reference level=0.05 m; settling velocity $w_{sand}=0.02$ m/s; scaling coefficient current-related mixing $\beta=1$ (default); density: sediment density $\rho_s=2650$ kg/m³; fluid density $\rho_w=1020$ kg/m³, kinematic viscosity coefficient $\nu=0.000001$ m²/s.

Figure 6.6 shows the measured water depths, measured depth-mean velocities, measured suspended transport rates and the computed suspended transport rates based on the SUSTIM2DV-model. The scaling coefficient of the bed concentration is set to 1.5 (default=1) to obtain the best agreement compared to the measured sand transport values. The computed suspended sand transport is somewhat too high at the highest current velocities of 1.7 to 1.8 m/s and somewhat too low at velocities below 1.5 m/s, but on average a good results is found in comparison with the measured values. Based on this, it is concluded that the SUSTIM2DV-model produces realistic sand concentrations and transport values.

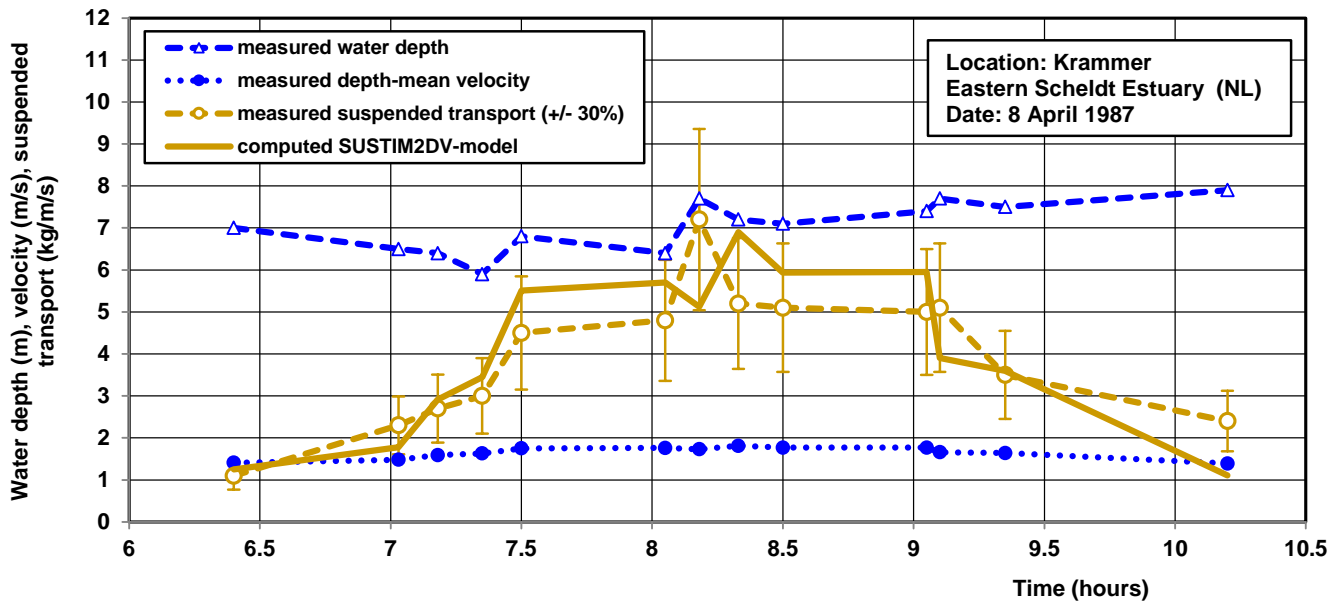


Figure 6.6 Measured and computed suspended sand transport, tidal channel Krammer, 1987, Eastern Scheldt, The Netherlands

7. References

Termes, 1990. *Sedimentation channels Rotterdam harbour (in Dutch)*. Report Q 1109, Delft Hydraulics, Delft, The Netherlands

Van Ledden, M., 2003. *Sand-mud segregation in estuaries and tidal basins*. Doctoral Thesis, Department of Civil Engineering, Delft University of Technology, Delft, The Netherlands

Van Rijn, 1993. *Principles of sediment transport in rivers, estuaries and coastal seas*. www.aquapublications.nl

Van Rijn, L.C., 2007. *Unified view of sediment transport by currents and waves, I, II, III*. ASCE, *Journal of Hydraulic Engineering*, Vol. 133, No. 6, 649-667, 668-689, No. 7, 761-775

Van Rijn 2006, 2012. *Principles of sedimentation and erosion engineering in rivers, estuaries and coastal seas*. www.aquapublications.nl

Van Rijn, L.C., 2011. *Principles of fluid flow and surface waves in rivers, estuaries and coastal seas*. www.aquapublications.nl

Van Rijn, L.C., 2023. *Modelling of sand and mud transport in tidal flow; SUSTIM2DV-model*. www.leovanrijn-sediment.com

Voogt, L., Van Rijn, L.C. and Van den Berg, J.H., 1991. *Sediment transport of fine sands at high velocities*. *Journal of Hydraulic Engineering*, ASCE, Vol. 117, No. 7.